2020

Mechanisms underlying variable responses to the neuropeptide C-type allatostatin (AST-C) across isoforms and among individuals in the American lobster, *Homarus americanus*

Audrey J. Muscato
Bowdoin College

Mechanisms underlying variable responses to the neuropeptide C-type allatostatin (AST-C) across isoforms and among individuals in the American lobster, *Homarus americanus*

An Honors Project for the Program of Neuroscience

By Audrey J. Muscato

Bowdoin College, 2020

Table of Contents

Acknowledgements

First and foremost, I would like to thank my mentor and advisor, Patsy Dickinson. Patsy, without your guidance over the years, I would not be where I am today. You inspired me to dedicate much of my time at Bowdoin to this research project and it has been one of the most rewarding parts of my experience, giving me a love of research and science that I did not know I could have. You have set an incredible example for what a mentor should be and I will spend my future career trying to emulate all that you have taught me.

Additionally, I was lucky to have a number of secondary advisors on this project. I would like to thank Andy Christie and Joel Graber for their work and guidance as I immersed myself in the foreign world of transcriptomics and bioinformatics. Furthermore, during my time at Bowdoin, I have found Druckenmiller Hall to be a place where there is always someone eager to listen to you talk about your research and provide input where they can. Professors Hadley Horch and Jack Bateman are two people who make Druck as welcoming as it is. Thank you for your guidance on this project, and for your lectures, which have shown me what it means to be excited by science. I'd also like to thank the people that make Druck tick, including Marko Melendy and Martha Mixon for their work in animal caretaking and instrumentation.

One of the most enjoyable parts of my research in the Dickinson lab has been the people I have met along the way. To my summer lab mates, thank you for making me laugh and for always being willing to accompany me to the C-store for Airheads and Raspberry Rosé seltzer. To my fellow Class of 2020 honors students, thank you for fostering a community of support and encouragement. I also had the opportunity to conduct some of the research for this project at Mount Desert Island Biological Laboratory. So, I would like to thank Dave Schulz for travelling to Maine in March to be our fearless leader in all things qPCR, and Niki Bothwick for her work on the qPCR portion of this project and for being the ultimate lab partner.

This project would not have been possible without funding from the Arnold & Mabel Beckman Foundation, the National Institutes of Health and IDeA Network of Biomedical Research Excellence (award P20GM0103423 from NIGMS), and the National Science Foundation (award IOS-1354567).

Finally, I would not be anywhere near the student or person I am today without the people who have supported me in every walk of life. To my siblings—Nate, Jake, and Gwen—thank you for always setting the bar high and believing without a shadow of a doubt that I would be able to match it. I cannot imagine who I would be without your love and support. To my parents, you have always believed in me, accepted me, and supported me unconditionally and for that I am eternally grateful. Thank you for being there and for raising me to be kind, be safe, and do the right thing. To Sophie, thank you for telling me that I could whenever I thought that I could not. I am so lucky to have you in my corner. To my wonderful friends, thank you— to Rohini, for breakfasts and lunches and late nights of both stress and laughter; to Olivia, for never failing to make me smile; to Carolyn, for listening when I needed to rant and talking when I needed to be distracted; and to Niki, for waiting for me in the Atrium and letting me be my truest self. To the people that Bowdoin College has given me, thank you for turning Brunswick into home more than I ever thought possible.

Abstract

Neuronal networks called central pattern generators (CPGs) produce patterned outputs independent of sensory input regarding timing. Unlike the myogenic human heart, the cardiac neuromuscular system of the American lobster (*Homarus americanus*) is neurogenic and driven by a CPG called the cardiac ganglion. The cardiac ganglion is composed of just nine neurons, making it a simple model system of study. Modulation of CPGs like the cardiac ganglion by neuropeptides allows for functional flexibility in the patterned output of the network. One neuropeptide family that modulates the cardiac system is C-type allatostatin. Three isoforms of this neuropeptide (AST-C I-III) have been identified. AST-Cs have the ability to alter both the frequency and amplitude of the crustacean heartbeat. Previous research has shown variation in the responses of the cardiac system both across the three isoforms and among individuals. This project aimed to understand the mechanisms underlying both of these types of variation.

First, we investigated why AST-C I and III elicit responses in both contraction frequency and amplitude that are more similar to each other than they are to the responses elicited by AST-C II. We hypothesized that a specific amino acid difference in the conserved sequence of the peptide was responsible for the observed variation in responses. To test this, we synthesized isoforms of AST-C that replaced the endogenous amino acid with that of another isoform and recorded physiological responses to the endogenous and synthetic isoforms. The results suggest that the identity of one particular amino acid in the conserved sequence is responsible for variations in responses in contraction frequency, and at least partially responsible for variations in responses in contraction amplitude.

The second component of this project focused on variation among individual animals in their responses to AST-C I and III. Perfusion of AST-C I and III through the cardiac system causes a wide range of responses among individual lobsters; some lobsters respond with a large

increase in contraction amplitude, while others respond with a large decrease. We hypothesized that the mechanism behind this variation is differential expression of four AST-C receptors and/or their downstream targets in the cardiac ganglion. To investigate these hypotheses, we recorded physiological responses of the cardiac system to AST-C I and III, then extracted and sequenced cardiac ganglion RNA from the same lobsters in order to analyze expression levels. Subsequently, we performed bioinformatic analysis on the sequenced data to determine if differential expression of AST-C receptors and downstream factors is correlated with the variation in responses to AST-C. Differential expression of one of the AST-C receptors (AST-CR 1) is correlated with physiological response. Furthermore, a number of downstream factors such as kinases and ion channels are differentially expressed in accordance with physiological response to AST-C. These findings propose potential mechanisms underlying individual variation and inspire further experimentation investigating molt cycle as the underlying cause.

Introduction

Project Overview

The goal of this project was to understand the mechanisms underlying two types of variation in responses of the American lobster (*Homarus americanus*) cardiac neuromuscular system: variation across isoforms of a modulatory neuropeptide and variation among individuals. The cardiac responses are characterized by changes in two parameters of the heartbeat—contraction amplitude and contraction frequency. These responses are the result of neuromodulation of the central pattern generator that controls the cardiac system by a family of neuropeptides called C-type allatostatins. Thus, this project used physiological, molecular, and bioinformatic techniques to understand the mechanisms underlying variation in responses to neuromodulation.

Central Pattern Generators

Central pattern generators (CPGs) are neuronal networks that produce rhythmic, patterned outputs without the need for sensory input. CPGs are found in both vertebrates and invertebrates and are responsible for various patterned behaviors such as locomotion and respiration (Dickinson, 2006). Evidence supporting the role of central pattern generators comes from work showing that—both *in vivo* and *in vitro*—the nervous system can generate rhythmic motor patterns. Isolated CPGs *in vitro* generate fictive motor patterns, which act in a way that would drive muscle movements if the muscles were still connected to the system (Marder and Bucher, 2001). Fictive motor patterns have been observed in a number of different preparations and are often similar to the patterns generated *in vivo*. However, differences do exist between some patterns *in vivo* and *in vitro*; this is largely due to the way sensory input pathways act on the CPG, even though CPGs are not dependent on this sensory input for pattern generation (Marder and Bucher, 2001).

The ability of CPGs to generate rhythmic patterns is largely due to the intrinsic properties of the neurons involved. Important intrinsic properties of the neurons include threshold and firing frequency (Getting, 1989). These properties can determine whether a neuron fires bursts of action potentials, generates plateau potentials, exhibits post-inhibitory rebound, or shows spike-frequency adaptation, which is when the frequency of action potentials decreases throughout a constant depolarization. Intrinsic neuronal properties, as well as synaptic factors such as strength and timing, dictate how a network functions overall (Marder and Bucher, 2001).

Researchers are particularly interested in how central pattern generators drive rhythmic behavior. There are two main mechanisms behind the rhythmic patterns generated by CPGs: either the network itself is driven by pacemaker neurons that have intrinsically patterned firing behaviors or the connections between neurons, which are not firing in a pattern themselves, can cause multiple neurons to produce a rhythmic pattern together (Marder and Bucher, 2001). Furthermore, the connection of CPGs to motor behavior can be dictated by premotor neurons within the system driving the activity of motor neurons outside the network, or by motor neurons that are directly active in generating the rhythmic firing pattern (Marder and Bucher, 2001).

Neuromodulation

Since central pattern generators are required for a number of functions and must adapt their patterned behavior to changing environmental demands, they must be functionally flexible. To accommodate this need, modulation of central pattern generators allows for flexibility in their typically fixed outputs. Neuropeptides commonly act as modulators of CPGs. Two general ways that modulators can change the firing of a central pattern generator are by altering intrinsic membrane properties like the plateau potential and by changing the strength of synaptic connections between different neurons (Marder and Bucher, 2001; Dickinson, 2006). Additionally, the stomatogastric ganglion (STG) of the American lobster (*Homarus americanus*),

which contains multiple central pattern generators, presents another method of modulation; modulators of the STG can reshape the many pattern generators, switching a neuron from one network to another. Modulators can be both fast-acting in the time it takes them to alter pattern generator output and long-lasting in the time that they exert an effect on the output (Dickinson, 1995).

Neuromodulators can come from a range of sources. The cardiac central pattern generator of the American lobster presents a few examples of the types of sources from which neuromodulators originate. For instance, dopamine can be released on the cardiac system from two different sources. Dopamine is produced in a large cell of the lobster's commissural ganglion that projects axons both directly to the cardiac ganglion—where dopamine can act locally—and to the pericardial organ—where dopamine can be released into the hemolymph and reach the heart indirectly through the circulatory system (Dickinson, 2006). Furthermore, the lobster cardiac ganglion also includes an example where a neuromodulator—in this case nitric oxide—is released from the target of the pattern generator: the cardiac muscles. After release, nitric oxide acts as a negative feedback messenger onto the cardiac ganglion itself (Mahadevan et al., 2004).

Lobster Cardiac Ganglion

Unlike the myogenic vertebrate heart, the crustacean heart is neurogenic; its contractions are controlled by the neurons that innervate the striated muscle fibers of a single ventricle (Yazawa et al., 1999). Severance of these nerves leads to the immediate cessation of contractions, demonstrating that the heart is completely neurogenic (Cooke, 2002). Hemolymph enters the heart from the lobster's open circulatory system through openings in the exterior of the heart called ostia. There are two pairs of ostia located in the dorsal wall of the heart and one pair located in the ventral wall. The hemolymph is pumped out of the ventricle through the arteries:

two posterior and five anterior (Figure 1). These contractions are controlled by a central pattern generator, which contains interneurons, as well as the motor neurons that innervate the muscle fibers (Yazawa et al., 1999).

In the American lobster (*Homarus americanus*), the CPG that controls the cardiac neuromuscular system is called the cardiac ganglion (CG) and is embedded in the dorsal wall of the heart (Figure 1). The output of the cardiac ganglion dictates the patterning of the contractions of the lobster heart through various parameters such as the frequency and amplitude of the heartbeat. The cardiac ganglion is a Y-shaped trunk composed of just nine neurons, five of which are motor neurons and four of which are pacemaker neurons. The five motor neurons project their axons outside of the ganglion, innervating the muscle fibers. On the other hand, the pacemaker neurons serve as interneurons that project their axons only within the cardiac ganglion. All of the neurons have dendrites that reach outside of the ganglion and receive input from muscles that are responsive to stretch, allowing the CG to respond to the degree to which the heart fills with hemolymph (Cooke, 2002). Because of how few neurons comprise the CG, it is an excellent model to study central pattern generators, which are much larger and more complex in vertebrates than they are in invertebrates.

The generation of action potential bursts in the cardiac ganglion is dictated by synaptic potentials that are induced in the motor neurons by the pacemaker interneurons. The firing of the motor neurons is synchronized. This synchronization is due to the motor neurons being electrically coupled to each other and receiving common synaptic inputs from pacemaker neurons (Kuramoto and Yamagishi, 1990). The posterior pacemaker neurons send impulses along their axons to the anterior motor neurons, which in turn generate impulses of their own. The motor neuron impulses are first generated by the more posterior motor neurons and followed

by impulses generated by the more anterior motor neurons, which are located farther up the branches of the Y-shaped cardiac ganglion (Cooke, 2002). Synaptic inputs between the neurons are both chemical and electrical (Kuramoto and Yamagishi, 1990). For instance, the pacemaker neurons communicate with the motor neurons via chemically-mediated synaptic input, but all of the neurons are also electrically coupled, which allows for synchronization of slow potential changes (Cooke, 2002).

Another key feature of the neurons that comprise the cardiac ganglion is their ability to produce a patterned burst when responding to just a simple stimulus. The mechanism that allows for this intrinsic bursting is the slow and sustained depolarization known as the driver potential. These driver potentials are triggered by depolarizations and gradual potentials from pacemaker cells. Driver potentials originate in the soma or the region of the axon nearby. Crustacean neurons do not generate action potentials in the soma, but rather only within the axon. Therefore, driver potentials are generated far from the trigger zone of the axon, where the initiation of action potentials occurs. Action potentials are generated as the result of the driver potential reaching the action potential initiation region of the axon (Cooke, 2002). Numerous currents that contribute to driver potential and pattern generation have been identified in the somata of the cardiac motor neurons. These currents include an L-type slow calcium current (I_{CaS}), a transient calcium current (I_{CaT}), a calcium-activated inward current (I_{CAN}), and a largely non-inactivating TTX-sensitive current that could be equivalent to a persistent sodium current (I_{NaP}) (Ransdell et al., 2013). Together, these currents comprise a complex mechanism by which the cardiac ganglion generates bursts of action potentials that, in turn, cause the beating of the lobster heart.

C-type Allatostatin

Like any central pattern generator, the cardiac ganglion is susceptible to modulation by neurohormones and peptides. This modulation alters the output of the CG and subsequently the

patterning of the lobster heartbeat, allowing it to adapt to changing environmental needs. One family of neuropeptides that modulates the output of the CG is the C-type allatostatin family (AST-C). Three isoforms comprise this family of neuropeptides: AST-C I (pQIRYHQCYFNPISCF), AST-C II (SYWKQCAFNAVSCFamide), and AST-C III (GNGDGRLYWRCYFNAVSCF) (Dickinson et al., 2018).

Allatostatins were originally identified in cockroaches and named for their function inhibiting the corpora allata endocrine glands, which synthesize juvenile hormone and are important for metamorphosis. Allatostatins are thought to be the arthropod form of somatostatins, which are human inhibitory neuropeptides that activate receptors with a similar structure to allatostatin receptors (Veenstra, 2009). There are three peptide families of allatostatins: A-, B-, and C-type. A-type allatostatins are characterized by their FGLamide C-terminus. B-type allatostatins are C-terminally amidated and characterized by the presence of tryptophan in the second and ninth amino acid position (Stay and Tobe, 2006). C-type allatostatins (AST-Cs) have a PISCF motif at the C-terminus, as well as a pyroglutamine-blocked N-terminus, and a disulfide bridge between the two cysteine residues at positions 7 and 14 (Dickinson et al., 2009). Since their discovery in insects, allatostatins have also been identified in other types of arthropods, including crustaceans. The first crustacean in which allatostatins were identified was the shore crab, *Carcinus maenas* (Duve et al., 1997). All three families of allatostatins have since been identified in crustaceans with C-type allatostatins being identified most recently in *Homarus americanus* and 24 other decapod species. These findings suggest that C-type allatostatins are well conserved across crustaceans. Furthermore, these neuropeptides are bioactive and function in modulating both the cardiac ganglion and the stomatogastric nervous system in *H. americanus* (Dickinson et al., 2009).

C-type Allatostatin Receptors

C-type allatostatin receptors were first identified in *Drosophila* as G-protein coupled receptors (GPCRs) that are the invertebrate homologs of mammalian somatostatin receptors. However, these GPCRs are not activated by somatostatin agonists, but rather by AST-C peptides (Kreienkamp et al., 2002). Previous work in the Dickinson lab with fluorescent ligand binding imaging has confirmed the interaction of AST-C with three crustacean AST-C receptors (AST-CR 1, 2, & 4). The full sequence of an additional AST-C receptor (AST-CR 3) has not yet been determined and, therefore, experiments to confirm its interaction with AST-C cannot be performed. The four AST-C receptors have a high degree of similarity (Walsh, 2017).

Crustacean AST-C receptors have been characterized as Class A or Rhodopsin-like G-protein coupled receptors (Walsh, 2017). This classification is based on the presence of several structural motifs characteristic of Class A GPCRs. Those structural features include seven transmembrane spanning helices, three extracellular and three intracellular loops, an extracellular N-terminal domain, and an intracellular C-terminal domain. The receptors each contain a disulfide bridge between the first and second extracellular loops, which is thought to function in stabilizing the transmembrane domains (Walsh, 2017). All four of the AST-C receptors also include N-glycosylation sites, which allow for post-translational modifications important for Class A GPCR function. Furthermore, AST-C receptors 1 and 2 both showed localization at the cell membrane in a cell line originating from the ovarian cells of the moth, *Trichoplusia ni*, which—like the American lobster—is a member of the phylum Arthropoda. Localization at the cell membrane is characteristic of Class A GPCRs. AST-C receptor 4 failed to show localization to the cell membrane, although this could have been due to complications with the enhanced-GFP experiment (Walsh, 2017).

Lobster Cardiac Responses to AST-C

The amplitude and frequency of the lobster heartbeat are modulated by perfusion of AST-C throughout the system. C-type allatostatins usually cause a decrease in contraction frequency, slowing the beating of the heart. However, the effects they have on contraction amplitude—the strength of the heartbeat—are more variable than the effects they have on contraction frequency (Wiwatpanit et al., 2012). In fact, all three isoforms (AST-C I, II, III) can elicit both increases and decreases in contraction amplitude. Previous research has shown variability in responses to AST-C across isoforms and among individuals (Figures 2 & 3) (Dickinson et al., 2018). This project investigated the mechanisms underlying these two types of variability in responses to AST-C.

First, responses of both contraction amplitude and frequency to AST-C show great variation across the different isoforms. AST-C I and III elicit responses that are more similar to each other than to those elicited by AST-C II. Because responses to AST-C peptides are highly variable, this variation across isoforms is most easily characterized by differences in the distributions of responses of multiple lobsters to the AST-C isoforms. AST-C I and III's distributions of responses are centered below zero; this means that the median responses of change in both amplitude and frequency are negative. Furthermore, the distributions of AST-C I and III have a wide range, including some hearts that respond with large increases in contraction characteristics and others that respond with large decreases. On the other hand, the distribution of responses to AST-C II is characterized by a narrower shape with less variability among lobsters and a less negative median for both percent change in frequency and amplitude (Figure 3; Dickinson et al., 2018). This shows that, as a whole, lobsters respond differently to AST-C I and III as compared to AST-C II. Therefore, the first aim of this project was to understand what

differences in the structures of the AST-C isoforms account for the variability in response distributions.

Second, there is great variation in contraction amplitude responses of individual lobsters to AST-C I and III (Dickinson et al., 2018). The wide distributions of responses to AST-C I and III show that some lobsters respond with a great increase in contraction amplitude, while others respond with a great decrease (Figures 2 & 3B). This individual variation is not easily explained by any obvious differences between the lobsters. Thus, this project aimed to identify the mechanism underlying why and how individual lobsters respond with such variability.

Variation across Isoforms

To investigate the different responses elicited by AST-C II compared to AST-C I and III, we focused on differences in the structures and sequences of the isoforms. There are a few structural variations between AST-C II and AST-C I and III. To start, AST-C II is amidated on the C-terminus of its peptide sequence, while AST-C I and III are not C-terminally amidated (Table 1). A structural variation like this could likely cause a different response in the cardiac system. In fact, differences in amidation states of neuropeptides have been shown to alter the bioactivity of other peptides in the CG (Stanhope, 2018). However, previous research has shown that differences in the amidation states of AST-C isoforms are not the cause of differences in response characteristics (Mackenzie, 2019; Rolph, 2019). This was determined by designing and synthesizing peptide isoforms that had the opposite amidation state as their endogenous counterparts (Table 1). A synthetic AST-C II without C-terminal amidation as well as synthetic AST-C I and III with C-terminal amidation were tested. This study found that amidation at the C-terminus was not responsible for the differences seen in responses to the various isoforms (Mackenzie, 2019; Rolph, 2019).

The next logical structural variant that we hypothesized is responsible for variability across isoforms was the amino acid difference within the conserved sequence of the peptide isoforms. In the conserved sequence, AST-C I and III have a tyrosine (Y) at the same position that AST-C II has an alanine (A) (Table 2). It should also be noted that an additional amino acid difference exists between AST-C II and AST-C I and III outside of the conserved sequence. In this position, AST-C I and III have a tyrosine while AST-C II has a tryptophan (W). However, because the alanine vs. tyrosine difference is located in the conserved sequence, we focused on it. Thus, we hypothesized that the differences in the response elicited by the isoforms are the result of the difference in amino acid identity at this position in the conserved sequence. Therefore, to test this hypothesis, we synthesized isoforms of AST-C II and III that have the amino acid at this position changed from the endogenous sequence (Table 2). For example, the synthetic AST-C II isoform—AST-C II Y—contains a tyrosine in the position that has an alanine in the endogenous form. The synthetic AST-C III isoform—AST-C III A—contains an alanine in the position that has a tyrosine in the endogenous form. We predicted that the responses of the heart to the isoforms with tyrosine in their conserved sequence would be more similar to each other than they are to the responses of the heart to the isoforms with alanine in their conserved sequence.

Variation among Individuals

The second question that this project aimed to answer was what molecular mechanism is responsible for the individual variation of the responses in amplitude to AST-C I and III. AST-C I and III can both cause some lobsters to strongly increase the contraction amplitude of their heartbeat and others to decrease the contraction amplitude (Figures 2 & 3). While it is natural to find variability among individuals in the magnitude of a response to a particular peptide, it is unusual to find such wide variability in the directionality of the response. Furthermore, a

previous study has shown that the changes in both amplitude and frequency in response to AST-C are not predictable based on the baseline parameters of the heartbeat before perfusion of the AST-C peptide (Dickinson et al., 2018).

First, it is important to note that lobsters that respond with an increase in amplitude show significant increases in the burst duration of the CG, suggesting that the mechanism underlying the effects of AST-C in modulating the pattern of the cardiac system is located in the cardiac ganglion (Wiwatpanit et al., 2012). Furthermore, four different receptors that mediate responses to C-type allatostatin have been found (Walsh, 2017). With this information in mind, we hypothesized that differential expression of the four AST-C receptors may underlie the variation seen in amplitude response to AST-C between individual lobsters. Another hypothesis is that factors downstream from the AST-C receptors—such as second messengers and ion channels—are differentially expressed among lobsters and responsible for the variability seen in response to AST-C isoforms. These hypotheses are not mutually exclusive, as it is possible that multiple factors are contributing to the individual variation in responses to AST-C I and III. Differential expression of AST-C receptors and any components of the pathways that they act on could potentially have an effect on the responses in amplitude to AST-C. In order to investigate these hypotheses, we combined physiological and transcriptomic techniques. The physiological responses of lobster cardiac systems were recorded and then the RNA of the cardiac ganglia of these same lobsters was sequenced. Then, we used bioinformatics to analyze the expression levels of AST-C receptors and other transcripts in each sample in an attempt to identify a mechanism underlying the individual variation among lobsters.

In addition to asking how the cardiac ganglion is modulated by AST-C with such great individual variability, we were also interested in why this is the case. One hypothesis is that

variation in amplitude of response to AST-C perfusion results from the lobster's molt stage. This hypothesis is based on the observation that many of the lobsters responding to AST-C with an increase in amplitude have appeared to be close to molting (Wiwatpanit et al., 2012; Dickinson et al., 2018). Therefore, we hypothesized that molecular indicators of molting—such as cryptocyanin and other members of the arthropod hemocyanin gene family (Terwilliger et al., 1999)—are more highly expressed in the RNA of lobsters that responded to AST-C with an increase in amplitude. This would tell us that the direction of the AST-C response is associated with the molt stage of the lobster and potentially with the differential expression of AST-C receptors or downstream factors that are the hypothesized mechanism behind this response.

Materials & Methods

Lobsters

American lobsters (*Homarus americanus*) were purchased in Brunswick, Maine and kept at Bowdoin College. Both male and female soft- and hard-shell lobsters were bought and used for experiments. The lobsters were housed in tanks of recirculating seawater kept at 10°C. The lobsters were kept on a 12-hour light, 12-hour dark cycle and fed chopped shrimp and squid weekly.

Peptides

Two C-type allatostatin peptides were synthesized in addition to the three endogenous AST-C isoforms. For the synthetic peptides, the amino acid of interest in the conserved sequence of one isoform was replaced with the amino acid from the other isoform (Table 2). Thus, the synthetic AST-C II Y isoform was synthesized with a tyrosine in the position of the conserved sequence that typically contains an alanine in the endogenous AST-C II. Conversely, the synthetic AST-C III A isoform was synthesized with an alanine in the position of the conserved sequence that contains a tyrosine in the endogenous AST-C III. A synthetic version of AST-C I containing an alanine (AST-C I A) was not synthesized for a few reasons. First, with AST-C III A, we were able to observe the effects of replacing a tyrosine in an endogenous isoform with an alanine, so AST-C I A would have been redundant in our analysis. Using only AST-C III A allowed us to minimize the cost associated with synthesizing isoforms. Furthermore, we chose to use a synthetic form of AST-C III instead of AST-C I because there is another position in the conserved sequence of the AST-C peptide where the isoforms differ. In this position, AST-C I has a proline, while AST-C II and III both have an alanine. Therefore, by comparing the synthetic and endogenous forms of AST-C II and III, the only difference in the conserved sequence was at the position of interest (tyrosine vs. alanine). All peptides were synthesized by

GenScript (Piscataway, NJ) and stored as a stock solution of 10^{-3} M at -20°C before being diluted to 10^{-7} M immediately prior to use.

Physiological Methods

The physiological responses of the lobster cardiac neuromuscular system to perfusion of C-type allatostatin isoforms were recorded. To do this, lobsters were anesthetized on ice for 30-60 minutes and then the lobster heart was removed from the body and kept in cold lobster physiological saline (composition in mM: 479.12 NaCl, 12.74 KCl, 13.67 $CaCl_2$, 20.00 $MgSO_4$, 3.91 Na_2SO_4, 11.45 Trizma base, and 4.82 maleic acid; pH 7.45) (Dickinson et al., 2018). The posterior artery was cannulated, so that saline could be perfused through the heart. The saline was kept cold (10-12°C) using a Peltier temperature regulator (CL100 bipolar temperature controller and SC-20 solution heater/cooler; Warner Instruments, Hampden, CT). The perfusion rate through the heart was held constant at 2.5mL/min by a Rabbit peristaltic pump (Gilson, Middleton, WI). The anterior arteries were tied to a FT03 force transducer (Grass Natus Technologies, Pleasanton, CA) which picked up the movement of the heart with each contraction, making it possible to calculate amplitude and frequency of the heartbeat. The output of the force transducer was amplified using an ETH-250 Bridge amplifier (CB Sciences, Dover, NH) with a high pass filter set to 4 Hz, and a Brownlee 410 instrumentation amplifier (Brownlee Precision, San Jose, CA). Contractions of the heartbeat were recorded at a sampling frequency of 10,000 Hz on a P.C. computer using a 1401 data acquisition interface and CED Spike2 software (Cambridge Electronic Design Limited). After a one-hour period of stabilization, each AST-C isoform was perfused through the system individually with 50-minute washes in between isoforms. For this project, five different AST-C isoforms were perfused through the heart (at 10^{-7} M concentration): the three endogenous isoforms (AST-C I, II, and III), as well as the two

synthetic isoforms (AST-C II Y and AST-C III A). Thus, the modulation of the heartbeat in response to each AST-C isoform was recorded.

Physiological Analysis

The physiological responses of the cardiac neuromuscular system to AST-C were analyzed by calculating the amplitude and frequency of the heartbeat over the course of the recording in Spike2 using functions built into the program. The percent changes in amplitude and frequency were then calculated by determining the average amplitude and frequency of a set of 50 heartbeats at baseline before the peptide was perfused, during the peak response of the heart to the peptide, and after the peptide had been entirely washed out and the heartbeat had returned to baseline amplitude and frequency. Only lobsters that recovered from all peptides were used in analysis. For the portion of the project investigating the variation across peptide isoforms, distributions of the percent changes in frequency and amplitude were generated for the four peptide isoforms in question: AST-C II, III, II Y, and III A. The responses of the heartbeat to the endogenous AST-C I were not used in analysis because there was no synthetic AST-C I A for comparison. The shapes of the distributions of responses were analyzed using Kolmogorov-Smirnov tests ($\alpha = 0.008$, Bonferroni's correction) and the means of the response distributions were analyzed using a one-way ANOVA test followed by post-hoc Tukey's multiple comparisons tests ($\alpha = 0.05$).

Molecular Methods

Four different tissues were dissected from the lobster: cardiac ganglion, eyestalk, hypodermis, and brain. The eyestalk, hypodermis, and brain were dissected after the heart was removed from the lobster, while the cardiac ganglion was dissected out of the heart after physiological recording was complete. Tissues were stored in RNA Later until RNA was extracted from each tissue using Direct-zol RNA Kits (Micro Prep for the CG and Mini Prep for the other tissues).

The quality and quantity of the RNA was confirmed using an Agilent 2100 Bioanalyzer or 4150 TapeStation bioanalyzer instrument (Agilent Technologies, Santa Clara, CA). The extracted RNA was stored at -80°C until further use.

Illumina RNA-Sequencing

Paired-end Illumina RNA Sequencing was performed by Georgia Genomics at the University of Georgia (Athens, GA) on the RNA from the cardiac ganglia of 24 different lobsters for which the physiological responses to AST-C I and III had been recorded. The 24 lobsters were chosen because they represented a wide distribution of responses in contraction amplitude to AST-C I and III (Figure 4). They were also chosen because their RNA was of high quality and therefore suitable for sequencing.

Bioinformatics

All programs used in the bioinformatic workflow of the Illumina RNA-Sequencing data were run on the Bowdoin College Computing Grid (server name: moosehead) and are summarized in Table 3. Quality control checks were performed on the sequencing data obtained from Georgia Genomics using FastQC, a program that analyzes sequencing data against various quality measurements. After the reads were run through FastQC, it was evident that there were quality issues based on an error made by the sequencing company, so the data were cleaned using Trimmomatic. Strict Trimmomatic parameters were required to eliminate the worst quality reads from the data. Those parameters removed any bases at the beginning or end of the reads if their quality score was below three, set a target length of forty bases using the "Max.info" function, and eliminated any reads that had an average Phred Score below 28 or were shorter than 25 bases long. This process removed 20-25% of the reads due to low quality. After the data were cleaned using Trimmomatic, FastQC was used again to confirm the quality of the remaining reads.

After passing a second quality control check, the data were pseudoaligned and aligned to four different American lobster transcriptomes using the programs Kallisto and Bowtie2, respectively. The four transcriptomes used were a cardiac ganglion transcriptome (Accession Number: GGPK00000000; BioProject Number: PRJNA412549), a brain transcriptome (Accession Number: GFUC00000000; BioProject Number: PRJNA379629), an eyestalk transcriptome (Accession Number: GFDA00000000; BioProject Number: PRJNA338672), and a mixed neural tissue transcriptome (Accession Number: GEBG00000000; BioProject Number: PRJNA300643) (Christie et al., 2015; Christie et al., 2017; Christie et al., 2018b; Christie et al., 2018a). The Kallisto pseudoalignments generated tables of estimated counts of reads and transcripts per million that aligned with each transcript in the transcriptome.

Concatenating Transcriptomes

After preliminary analysis, it became clear that in order to maximize the read coverage of the reference transcriptome it was necessary to combine the four transcriptomes into one. The methodology used to concatenate the transcriptomes was derived from Cerveau and Jackson (2016). Before the transcriptomes were concatenated, the redundancies of each transcriptome were reduced using the CD-HIT-EST program. CD-HIT-EST organized transcripts into clusters based on similarity; each cluster was then classified as a single representative sequence. CD-HIT-EST clustered 67,690 transcripts from the mixed neural tissue transcriptome into 67,334 clusters, 146,106 transcripts from the eyestalk transcriptome into 102,718 clusters, 150,579 transcripts from the brain transcriptome into 106,998 clusters, and 189,952 transcripts from the cardiac ganglion transcriptome into 127,191 clusters.

After CD-HIT-EST, the clustered transcriptomes were run through TransDecoder which identifies the likeliest open reading frames (ORFs) in a transcript. The ORFs identified by TransDecoder were pulled out from the CD-HIT-EST clustered transcriptomes and all four

collections of the most likely ORFs were concatenated together to create one combined transcriptome. The combined master transcriptome was run through CD-HIT-EST again in order to reduce redundancies that arose from combining four different transcriptomes.

This master transcriptome was annotated by aligning the sequences of the transcripts to the known protein identities in *Drosophila melanogaster*. This was done by running the nucleotides of the lobster master transcriptome through blastx against a database of all of the annotated proteins in *Drosophila*. Thus, the transcripts in the master lobster transcriptome were annotated based on their similarity to those in *Drosophila*.

Aligning to the Master Transcriptome

The RNA-Sequencing data from the cardiac ganglia of the 24 different lobsters were then mapped to the master transcriptome for reference. This pseudoalignment was performed by Kallisto. Kallisto generated estimated count and transcripts per million (tpm) data on the expression of each of the transcripts from the transcriptome in the cardiac ganglion RNA samples.

Spearman Correlations of AST-C Receptors

Spearman correlations were performed in R to analyze the relationship between the expression of AST-C receptors 1-4 and the physiological response to AST-C I. In addition to analyzing the expression of individual receptors, the ratio of expression of each receptor to every other receptor was calculated for each sample. Spearman correlations were performed to analyze the relationship between these ratios and the physiological responses.

Principal Component Analysis

Principal component analysis (PCA) was performed in JMP software (Version 13) to determine what factors might be driving differential expression of transcripts within the samples. A correlation was performed to determine how strongly correlated the physiological responses of the heart to AST-C I and the RNA expression levels were. This PCA was also used to pull out

networks of genes that were upregulated or downregulated with the principal component. Gene Ontology (GO) terms were then identified for these subsets of genes in order to understand their molecular functions.

Differential Expression Analysis

Differential expression analysis was performed using the DESeq2 program in R. The purpose of this analysis was to determine the fold changes in expression levels of each transcript between samples, which were organized based on their physiological response to AST-C I. Since the physiological response to AST-C I is a continuous variable and not a categorical one, the fold changes represent the slope of the correlation between expression of that transcript and AST-C I physiological response. This method of analysis is an alternative approach to the principal component analysis. Differential expression analysis generated a list of 615 transcripts that were differentially expressed (adjusted p-value < 0.10) based on physiological response to AST-C I perfusion.

Identification and Analysis of Differentially Expressed Transcripts

The 615 differentially expressed transcripts were identified through annotation based on alignment to three different databases of identified genes and proteins: FlyBase, SwissProt, and Hmmer. Due to the evolutionary similarity between *Homarus americanus* and *Drosophila* (which are both members of the phylum *Arthropoda*) and the extensive knowledge of the *Drosophila* genome, the transcripts that were identified by matching to *Drosophila* homologs were used for further analysis. The transcripts matched to *Drosophila* that were associated with an increase in contraction amplitude of the heartbeat and a decrease in contraction amplitude were separately entered into Gene Ontology software and biological process GO terms were generated. Based on GO terms relevant to neurophysiological functions, a list of genes that are up- and downregulated with physiological response was created. These genes of interest were

further investigated in *Drosophila* literature and FlyBase in order to understand their function, the pathways in which they act, and if they could be potentially targeted within the lobster through pharmaceutical intervention.

RT-qPCR of AST-C Receptors

In order to characterize the distribution of the four AST-C receptors across cell types in the cardiac ganglion, RT-qPCR was performed on the AST-C receptor transcripts in the motor neurons and the pacemaker neurons separately. First, the cardiac ganglia of eight lobsters (4 male, 4 female) were dissected and the areas containing the motor neurons and pacemakers were separated from each other. The tissues were then placed into 300 μL of lysis buffer. RNA was extracted from the neurons using the Quick-RNA Microprep Kit (Zymo Research). The extracted RNA was reverse transcribed into cDNA using the Invitrogen SuperScript III kit. SsoAdvanced PreAmp Supermix (Bio-Rad Laboratories) was used for the pre-amplification step. RT-qPCR was performed using primers designed with Integrated DNA Technologies specific to the four AST-C receptors: AST-CR 1 (5' CAGCGGCTACCAAATGACATC 3'), AST-CR 2 (5' GACGTCCCTCACGCTCATAG 3'), AST-CR 3 (5' GGCAGCCAACACAACACATAC 3'), and AST-CR 4 (5' CCTGGTGTTCGCAATTCCTTTC 3'). Primer efficiencies were tested before RT-qPCR was performed. The RT-qPCR reaction consisted of 40 cycles of 95°C, 58°C, and 72°C all for twenty seconds. The reaction was run on a Stratagene Mx3000p machine at Mount Desert Island Biological Laboratories (Bar Harbor, ME).

Analysis of RT-qPCR results was performed by determining the C_t values of each receptor transcript in each tissue type. Furthermore, the C_t values were normalized to 18S ribosomal RNA expression levels to control across tissue samples. ΔC_t values were calculated by subtracting the C_t value for the 18S ribosomal RNA of a specific tissue from the C_t value for the gene of interest (AST-C receptor) in that tissue. $\Delta\Delta C_t$ values were not calculated because paired

T-tests were used since there were both motor neuron and pacemaker samples from each individual lobster and individual variation was known to exist in the responses of the lobster heart to AST-C. Paired T-tests and F-tests to compare variances were performed on the ΔC_t values in GraphPad Prism 8 (GraphPad Software, San Diego, CA) to compare the expression of each receptor between motor neurons and pacemakers.

Hypodermis and Eyestalk RNA-Sequencing

To investigate the hypothesis that a lobster's molt cycle corresponds with their physiological response to AST-C, a second dataset of lobster RNA was sequenced using Illumina technology. Throughout the molt cycle, molt-inhibiting hormone (MIH) is released from the sinus gland, a neurohemal organ within the eyestalk of decapod species (Chang, 1995; Chang and Mykles, 2011). Additionally, gene expression in the hypodermis—the tissue underlying the carapace—is regulated throughout the molt cycle, with molt-related genes peaking in expression during the pre-molt stage (Tom et al., 2014). Due to the importance of the eyestalk and hypodermis in the molting function of the lobster, samples of these tissues were sent for Illumina RNA-Sequencing by Admera Health Biopharma Services (South Plainfield, New Jersey). Library preparation was performed with the NEBNext Ultra II kit with Poly-A selection. The samples included 24 eyestalk RNA samples and 17 hypodermis RNA samples from lobsters that had their physiological responses to AST-C recorded. Therefore, these RNA-Sequencing data can be analyzed in order to investigate a possible relationship between molt stage of the lobster (i.e. molt-related gene expression) and physiological response to AST-C. This analysis will add another layer of understanding to the individual variation in AST-C physiological response by looking at why such great individual variation exists.

Results

Variation across Isoforms

Contraction Frequency

In looking at the variation in response across isoforms of AST-C, it was hypothesized that the presence of a specific amino acid (either tyrosine or alanine) in the conserved sequence accounted for the variability. Therefore, in the analysis of the responses to the different peptide isoforms, we focused on comparing responses to the endogenous AST-C II and III, which contain alanine and tyrosine respectively, to the synthetic isoforms AST-C II Y (which has a tyrosine) and AST-C III A (which has an alanine). Perfusion of the four AST-C isoforms (AST-C II, III, II Y, and III A) caused a decrease in contraction frequency of the heart in most lobsters. Every isoform except AST-C III A caused a significant negative mean decrease in frequency (Figure 5; One-sample T-tests). Mean changes in frequency caused by AST-C II Y, AST-C II, and AST-C III were -19.20%, -8.53%, -19.30%, respectively. AST-C III A, on the other hand, did not elicit a significant change from baseline with a mean response of 0.48%. Each of the isoforms also elicited a fairly wide range of responses (Figure 6).

The responses of the cardiac system to the synthetic AST-C isoforms (AST-C II Y and AST-C III A) suggest that the specific amino acid partially explains the difference in contraction frequency responses to AST-C isoforms. The isoforms that have tyrosine in their conserved sequences elicited distributions of responses that are wider and more negatively centered in comparison to the distributions of responses elicited by isoforms with alanine in their conserved sequences (Figure 6). Replacing the amino acid in the endogenous isoform with the opposite amino acid affected both the shape and the center of the distribution. The responses of the lobster hearts to AST-C II and AST-C II Y differed significantly from each other in both mean percent change and shape of the distribution (Table 4). By replacing the alanine in the conserved sequence with a tyrosine, the distribution of the responses to the AST-C II Y isoform was shifted

more negatively than the distribution of the responses to the endogenous AST-C II. Furthermore, the endogenous AST-C III and the synthetic AST-C III A also elicited significantly different responses in frequency (Table 4). The replacement of the tyrosine in AST-C III with an alanine resulted in AST-C III A having a narrower distribution centered closer to zero.

Thus, the identity of the amino acid in this position of the conserved sequence has an effect on the responses in frequency to the isoform. The responses in frequency elicited by AST-C II Y are more similar to the responses elicited by AST-C III than to those elicited by AST-C II (Table 4). Although the same is not true statistically for AST-C III A and AST-C II, the responses to AST-C III A still appear to be more similar to the responses to AST-C II than to responses to AST-C III (Figure 6). These data suggest that whether the isoform has alanine or tyrosine in the conserved sequence has an effect on the change in frequency that it elicits. Broadly, isoforms with tyrosine more often caused decreases in frequency and were also subject to greater variability across individuals. On the other hand, isoforms with alanine generally had a smaller mean effect with less individual variation.

Contraction Amplitude

Perfusion of the four AST-C isoforms caused a range of effects in the amplitude of the heartbeat. None of the four AST-C isoforms caused a mean percent change in contraction amplitude that differed significantly from zero (Figure 7). Mean changes in contraction amplitude caused by AST-C II Y, II, III and III A were 0.13%, 2.20%, -2.77%, -0.69%. While the mean percent changes were all relatively close to zero, AST-C II Y and III (which contain tyrosine) elicited a wide range of responses across individual lobsters, but AST-C II and III A (which contain alanine) had less variation in response (Figure 8). The ranges of the responses in amplitude to AST-C II Y, AST-C II, AST-C III, and AST-C III A were 83.09%, 45.71%, 60.53%, and 20.93%, respectively.

The responses in amplitude to the endogenous and synthetic AST-C isoforms suggest that the identity of the amino acid of interest had a nonsignificant effect on the responses elicited by AST-C II and III. The replacement of the alanine in the conserved sequence of AST-C II with a tyrosine (to make AST-C II Y) caused the isoform to elicit a much wider range of responses in amplitude. Conversely, the replacement of the tyrosine in the conserved sequence of the endogenous AST-C III with an alanine caused AST-C III A to elicit an apparently narrower range of responses in amplitude (Figure 8). However, the distributions of the endogenous and synthesized isoforms were not significantly different based on the Kolmogorov-Smirnov tests, except in the case of the two endogenous isoforms: AST-C II and AST-C III (Table 5). These data suggest that the presence of either alanine or tyrosine in the conserved sequence of the AST-C isoform had a slight, nonsignificant effect on amplitude response. Similar to the frequency data, the presence of tyrosine in the conserved sequence seemed to result in a wider range of responses across individuals.

Variation among Individuals

All of the RNA-sequencing data and physiological response data analyzed with regards to the individual variation research question were obtained from the 24 lobsters that had their cardiac ganglion RNA sequenced by Georgia Genomics. The physiological responses of these lobsters are shown in Figure 4.

AST-C I & III Correlation

Before analyzing the RNA-sequencing data, a Spearman correlation analysis was performed to analyze the relationship between the percent changes in amplitude of the heartbeat to AST-C I and AST-C III. The two physiological responses had a strong positive correlation, meaning that lobsters had similar individual responses to the two isoforms (Figure 9). This correlation suggests that the factors driving the direction of the amplitude response to one isoform also drive

the direction of the amplitude response to the other isoform. With this information, bioinformatic analysis of the RNA-sequencing data could be performed in order to investigate if differential expression of various transcripts is the mechanism underlying individual variation in response to AST-C I and III; this mechanism could be predicted by a correlation between transcript expression and physiological response. Because of this, we used the physiological response to one of the isoforms (AST-C I) as the variable tied to differential expression.

AST-C Receptors

First, Spearman correlations were performed on the expression of the various AST-C receptors and the physiological response to AST-C I. The intent of this analysis was to test one of the primary hypotheses: differential expression of AST-C receptors was responsible for individual variation in response. The expression of AST-C receptor 1 had a significant negative Spearman correlation ($R = -0.5$, $p = 0.012$) with the response in amplitude to AST-C I. This indicates that 50% of the variation in response is due to differential expression of AST-C receptor 1 (Figure 10A). However, the other three receptors did not show significant correlations between their expression levels and the physiological response (Figure 10B-D). Therefore, differential expression of AST-C receptor 1 may be a factor in determining the direction of the amplitude response to AST-C I, but the expression levels of the other receptors on their own do not seem to be a factor.

In order to investigate if the mechanism of differential expression relied on the relative expression of the receptors to each other, Spearman correlations of receptor expression ratios to AST-C I physiological response were performed. The ratio of expression of AST-C receptor 1 to receptor 4 showed a slight, non-significant correlation with physiological response to AST-C I (Figure 11). This indicates that, while not significant on their own, the expression levels of AST-C receptor 4 could be involved in the mechanism determining the directionality of the response

alongside AST-C receptor 1 expression levels. Spearman correlations were performed to analyze the relationship of the receptor expression ratios of every combination and of each receptor to total AST-C receptor expression, but none of the other correlations neared significance.

Principal Component Analysis

Since we hypothesized that differential expression of factors downstream from the receptors might also be partly responsible for individual variation in AST-C response, the next step was to perform a principal component analysis. PCA represented a different method of looking at the extent to which differential expression might be related to individual variation in response. The first principal component showed a modest negative correlation (R= -0.39) with the physiological responses to AST-C I. This suggests that response to AST-C I was the factor accounting for the most variability in the dataset. The principal component analysis also generated a list of transcripts that are upregulated with increased amplitude responses and a list of transcripts that are downregulated with increased amplitude response. The transcripts were identified based on sequence similarity to human genes. Molecular function Gene Ontology (GO) terms of the subsets of genes that were both up- and downregulated with physiological response to AST-C I are shown in Figures 12 and 13.

Differential Expression Analysis

An alternative method to understanding which transcripts may be affecting physiological response was to perform a differential expression analysis. This serves to pull out the transcripts that are differentially expressed between samples based on the physiological responses of the lobsters to AST-C perfusion. Differential expression analysis using DESeq2 led to the identification of 615 transcripts that are either significantly upregulated or downregulated (adjusted p-value < 0.10) with increasing AST-C I physiological response (Figure 14). 140 of the significantly differentially expressed transcripts were positively correlated with AST-C response,

while 475 were negatively correlated. This analysis was performed without one sample that was identified as an outlier dominating the second principal component. Next, the differentially expressed transcripts needed to be identified in order to understand the meaning of these results and how the molecular mechanism functions.

Analysis of Identified Differentially Expressed Transcripts

The significantly differentially expressed transcripts were identified by aligning them to three different annotated databases: FlyBase, SwissProt, and Hmmer. Due to the evolutionary similarity between *Drosophila* and *Homarus americanus*, the transcripts aligned to FlyBase were selected for further investigation. While *Drosophila* is the closest related species with a reference database, it is important to remember that it is still evolutionarily distant and thus a reference genome of *Homarus americanus* or another crustacean would be more effective for comparison if one were available. The differentially expressed transcripts that had expression levels positively correlated with change in contraction amplitude in response to AST-C I aligned to 389 FlyBase genes and those that were negatively correlated with change in contraction amplitude aligned to 361 FlyBase genes (Appendix A). These numbers of genes are different from the numbers of differentially expressed transcripts as some of those transcripts did not match to FlyBase and some matched to multiple FlyBase genes.

After identifying the transcripts that were significantly differentially expressed, the FlyBase identifiers for the matched transcripts were entered into Gene Ontology to perform GO term analysis on the transcripts that were positively or negatively correlated with increasing AST-C physiological response. These analyses provided a broader understanding of the biological processes that were either up- or downregulated in the cardiac ganglia of lobsters that had increases in contraction amplitude in response to AST-C perfusion. The complete list of enriched GO terms associated with all of the differentially expressed transcripts matched to

FlyBase is available in Appendix B. Out of the numerous GO terms that were returned from the analysis as being associated with the transcripts either up- or downregulated with increasing contraction amplitude in response to AST-C, those GO terms that were relevant to the physiological functions that control the cardiac ganglion's output were selected for further analysis (Figures 15 and 16).

Among the GO terms associated with the transcripts that are positively correlated with increasing contraction amplitude in response to AST-C, there are a selection of terms relevant to second messenger cascades and protein phosphorylation (Figure 15). AST-C receptors are G-protein coupled receptors and thus likely act through second messenger cascades to regulate the activity of the neurons in the cardiac ganglion through the phosphorylation and dephosphorylation of a variety of proteins. These proteins could include ion channels, phosphorylation of which could alter their conductance or voltage-dependence and therefore change the electrical activity of the neurons. Investigation of these GO terms, such as "activation of protein kinase activity" and "positive regulation of JNK and stress-activated MAPK cascades," led to the identification of a number of genes of interest that could be involved in the mechanism underlying individual variation in response to AST-C (Appendix C). The upregulation of kinases—including Gck III ortholog, Slik, Hippo, and Happyhour—in samples that had increases in contraction amplitude in response to AST-C presents a possible mechanism for individual variation. These are all serine/threonine kinases that act in a variety of pathways, including the Hippo pathway. It is unclear from these results exactly what targets these kinases are phosphorylating, but their increased activity suggests that they are working to activate or deactivate proteins associated with the cardiac response to AST-C. Therefore, their differential

expression could be important in determining the response to AST-C that the cardiac ganglion of a given lobster may show.

In addition to the kinases, there are a number of other positively-correlated transcripts that are relevant to the cardiac ganglion. One transcript that stands out is Alg2, which functions in calcium ion binding. This is of note because of the prominent role of calcium ions in the neuronal activity of the CG. Other positively-correlated transcripts are directly related to the idea of a signal transduction cascade from a G-protein coupled receptor. For instance, the alpha subunit of a G_o protein is interesting because of our prior knowledge that the AST-C receptors are G-protein coupled receptors. Perhaps the receptors act through the G_o alpha subunit to propagate a signal throughout the CG.

Fewer GO terms were associated with the negatively-correlated differentially expressed transcripts. Out of all the GO terms that the analysis returned (Appendix B), the ones of interest given the context of the cardiac ganglion were "response to external stimulus," "synapse organization," and "manganese ion transport" (Figure 16). These GO terms were all upregulated in samples that had decreases in contraction amplitude. While manganese ions are not relevant to the cardiac ganglion, one of the transcripts associated with this GO term is a transient receptor potential protein, which is a non-selective cation channel that has high calcium ion permeability (Appendix C). Calcium is an important ion in the cardiac ganglion as it is the basis of the cardiac ganglion's driver potential. Therefore, it is possible that differential expression of this receptor, as well as Toll-like receptors, could be an underlying mechanism in the individual variation in response to AST-C. Additionally, transcripts that are related to second messenger cascades are also present in the negatively-correlated group and could be acting in opposition to those in the positively-correlated group. These transcripts include a tyrosine-specific phosphatase, kinases,

and transmembrane signaling proteins (Notch and Klingon). More research will have to be conducted to fully elucidate the roles that these differentially expressed transcripts are playing, but many of them strongly implicate the differential expression of members of a second messenger cascade as being involved in the individual variation in response to AST-C.

RT-qPCR of AST-C Receptors

In order to investigate the distribution of AST-C receptors across the different cell types of the cardiac ganglion, RT-qPCR was performed on the transcripts for the four receptors separately in the two cell types (motor neurons and pacemakers). ΔC_t values were calculated for each sample (either pooled motor neurons or pacemakers for each lobster) by normalizing to 18S ribosomal RNA expression. None of the four AST-C receptors differed in average expression level between motor neurons and pacemakers (Paired T-tests, α=0.05, AST-CR 1: $p = 0.6107$, AST-CR 2: $p = 0.5968$, AST-CR 3: $p = 0.6340$, AST-CR 4: $p = 0.9745$). However, the variance of the receptor expression (measured by ΔC_t values) between motor neurons and pacemakers differed for all four receptors (F-tests for variance, α=0.05, AST-CR 1: $p = 0.0023$, AST-CR 2: $p < 0.0001$, AST-CR 3: $p = 0.0042$, AST-CR 4: $p < 0.0001$). The motor neurons had greater individual variation in expression of each AST-C receptor across lobsters (Figure 17).

Although the physiological responses of these lobsters to AST-C were not measured and a correlation therefore cannot be made between receptor expression in the motor neurons and physiological response, this finding is particularly interesting due to the nature of AST-C response having great individual variation. Since there is great individual variation in the expression of AST-C receptors within the motor neurons only, it is possible that this differential expression underlies the individual variation in physiological response. This could further explain why differential expression of receptors was not found to be as important as predicted in determining the physiological response of the lobster cardiac system to AST-C in the RNA-

Sequencing experiments and analysis because those data were collected from entire cardiac ganglia, not separated by cell type. In order to elucidate if variation in receptor expression across motor neurons of the cardiac ganglion is responsible for individual variation in physiological response to AST-C, further experiments would have to be performed in which a direct correlation between physiological response and receptor expression in the motor neurons could be measured. Nevertheless, these preliminary data allow us to refine our original hypothesis and help us to interpret the findings from the RNA-Sequencing analysis of receptor expression.

Discussion

This project investigated two types of variation observed in the responses of the *Homarus americanus* cardiac neuromuscular system to C-type allatostatin neuropeptides. First, it was hypothesized that differences in the responses of the cardiac system to the three isoforms of AST-C was due to a single amino acid difference in the conserved sequence of the peptide. Second, it was hypothesized that individual variation in the responses to AST-C among lobsters was caused by differential expression of AST-C receptors and associated downstream factors such as second messengers and ion channels. These questions are relevant to an overall understanding of mechanisms of variation in responses to neuropeptides within crustaceans and, more broadly, across all of biology.

Variation across Isoforms

The physiological responses of the various AST-C isoforms, both endogenous and synthetic, suggest that the amino acid difference between AST-C II and AST-C I and III in the conserved sequence of the peptide may be responsible for determining the change in frequency and amplitude of the heartbeat. These results suggest that the mechanism underlying the variation of responses across AST-C isoforms is heavily related to ligand-receptor interactions. This project asked what specific part of the ligand (AST-C) is most important in determining its interaction with receptors. Post-translational modifications, such as amidation, have been shown to alter the bioactivity of neuropeptides within the cardiac neuromuscular system of the American lobster (Stanhope, 2018). Furthermore, Mazarguil et al. (2001) showed that C-terminal amidation of Neuropeptide FF—which is involved in pain transmission in mammals—confers high affinity and activity in the interaction with the associated G-protein coupled receptors. However, previous research in the Dickinson lab investigating C-terminal amidation of AST-C isoforms has shown that amidation is not responsible for the observed differences across isoforms of C-

type allatostatin (Mackenzie, 2019; Rolph, 2019). While neuropeptide C-terminal amidation is responsible for changes in bioactivity in a variety of systems, it is not the driving factor for the differences in the activity of AST-C isoforms.

To further investigate the cause of different responses to the AST-C isoforms, we turned to specific amino acid differences in the peptide. Changes in amino acid residues in ligands have been shown to affect ligand-receptor interactions (Ackers and Smith, 1985). For instance, a single nucleotide polymorphism (SNP) of neuropeptide S—a vertebrate neuropeptide involved in a variety of physiological functions—that results in a non-synonymous amino acid substitution leads to significantly lower bioactivity compared to the wild type version (Deng et al., 2013). Therefore, the non-synonymous difference of alanine and tyrosine in the conserved sequences of the AST-C isoforms is also a potential cause of differences in bioactivity.

This project looked specifically at the consequences of whether an alanine or a tyrosine is present in the conserved sequence of the AST-C isoform. Alanine is a small, nonpolar, and slightly hydrophobic amino acid with an aliphatic side chain. It is often not involved in protein interactions, but it does function in substrate recognition. On the other hand, tyrosine is partially hydrophobic and is thus often found within a protein's hydrophobic core. It has an aromatic side chain. While alanine and tyrosine are both at least slightly hydrophobic, they are very different in their structure and function. The replacement of alanine with similar small amino acids typically does not cause a large effect in protein function. Similarly, the replacement of tyrosine with other aromatic amino acids does not affect protein function drastically (Betts and Russell, 2003). However, since alanine and tyrosine are not similar to each other, we expected the replacement of one for the other to have an effect of the function of the AST-C peptide. Therefore, the observed effects of the presence of alanine or tyrosine in the conserved sequence of AST-C on

the responses of the lobster heart are consistent with our hypothesis. Since tyrosine seems to cause the isoform to elicit a wider range of responses, it is possible that the presence of this amino acid alters the affinity of the AST-C neuropeptide to its receptors.

Going forward with this portion of the project, additional data should be collected to completely characterize the distributions of responses elicited by the endogenous and synthetic AST-C isoforms. There still remains the potential to investigate if a synthetic isoform of AST-C I containing alanine in its conserved sequence—AST-C I A—elicits similar responses from the cardiac system to the responses elicited by AST-C II. This investigation would further confirm the effects of the tyrosine vs. alanine difference in all three AST-C isoforms, as opposed to just AST-C II and III. Furthermore, a second amino acid difference exists between AST-C II and AST-C I and III; AST-C II has a tryptophan in its sequence where AST-C I and III have a tyrosine (Table 1). This difference is located outside of the conserved sequence and thus was not our first hypothesis for affecting response. However, it is possible that both differences in the sequences are responsible for the observed differences in response. Therefore, another potential step going forward would be to synthesize isoforms with both amino acids replaced for the ones in the opposite endogenous isoforms.

Overall, these data support our hypothesis and suggest a role of the presence of tyrosine at this specific location of the conserved sequence causing the AST-C isoform to have a more negatively centered distribution of frequency responses with a wider shape. This finding is consistent with other studies that have shown a change in bioactivity in peptides with SNPs leading to non-synonymous amino acid substitutions (Ackers and Smith, 1985; Deng et al., 2013). Furthermore, the observed effects of the amino acid difference in the AST-C isoforms are relevant beyond crustaceans. These findings further our understanding of the bioactivity of

neuropeptides generally and present a mechanism by which mutations to neuropeptides or the presence of different isoforms in any system could affect the responses elicited by that neuropeptide.

Variation among Individuals

This project sought to determine the mechanism underlying individual variation in physiological response to AST-C through analysis of Illumina RNA-Sequencing data. We hypothesized that differential expression of receptors and downstream factors was responsible for the individual variation observed in responses. Physiological responses in amplitude to AST-C I are highly correlated with the first principal component of RNA expression in the cardiac ganglion, suggesting that there is an RNA expression-dependent mechanism underlying the wide individual variation seen in responses. Through differential expression analysis, Spearman correlations, and GO term analysis, a number of components of this RNA expression-dependent mechanism have been elucidated.

The primary hypothesis was that differential expression of the four AST-C receptors was the mechanism underlying individual variation in AST-C response. This hypothesis is partially supported by our findings, as AST-C receptor 1 expression is correlated with physiological response to AST-C I, but expression of the other receptors is not (Figure 10). This finding of differential receptor expression is consistent with other findings in the crustacean field. Garcia et al. (2015) identified and investigated expression levels of a crustacean cardioactive peptide (CCAP) receptor in the stomatogastric ganglion (STG) of the crab *Cancer borealis*. The CCAP receptor, which is a G-protein coupled receptor, was differentially expressed across neuronal types in the STG and the expression levels were correlated with the individual neuron's strength of response to CCAP. For example, the lateral pyloric (LP) neuron displayed high expression of the CCAP receptor along with larger current responses and higher sensitivity to low

concentrations of CCAP (Garcia et al., 2015). Furthermore, differential expression of CCAP receptors among individuals was also observed. Since CCAP is known to be an important regulator of molting behavior, this individual variation in expression was posited to be associated with the molt stage of the lobster (Garcia et al., 2015). Oliphant et al. (2018) also observed differential expression of a number of receptors—in this case, in the Y-organs, which are associated with molting function—across the molt cycle. Given this current knowledge, molt stage could be a potential explanation for the differential expression of AST-CR 1 among individuals.

To further investigate AST-C receptor expression in the cardiac ganglion, preliminary RT-qPCR experiments were performed comparing expression of the four putative receptors between the two cell types: the posterior pacemaker neurons and the anterior motor neurons. In the lobster cardiac ganglion, differential expression of myosuppressin receptors (MSR) has been shown between cell types, with MSR-II and MSR-III having higher expression in the motor neurons and MSR-IV having higher expression in the pacemaker neurons (Oleisky et al., 2020). Although the preliminary AST-CR RT-qPCR experiments did not find a difference in receptor expression levels between cell types, there was a difference in the variance in expression levels between cell types. The motor neurons showed much greater variance in expression of all four AST-C receptors among individuals than the pacemaker neurons. Going forward, additional RT-qPCR experiments using lobsters with known physiological responses could be useful in determining differences in receptor expression specific to the motor neurons. These differences in receptor expression could potentially have been masked by the design of this RNA-Sequencing study in which motor and pacemaker neurons were pooled together for expression data of the cardiac ganglion as a whole.

In addition to the receptor hypothesis, we hypothesized that differential expression of downstream factors—such as second messengers, protein kinases, and ion channels—is responsible for the individual variation in response to AST-C. Kreienkamp et al. (2002) first discovered receptors activated by C-type allatostatin in *Drosophila melanogaster*, describing the receptors as invertebrate homologs of mammalian opioid/somatostatin receptors. In this study, AST-C receptors were identified as G-protein coupled receptors (Kreienkamp et al., 2002). It was later confirmed that the AST-C receptors in crustaceans like *Homarus americanus* were also G-protein coupled receptors (Walsh, 2017). GPCRs activate G-proteins, which can then either act directly within the cell to elicit a specific response or activate a second messenger cascade in which molecules like cyclic AMP (cAMP) and calcium ions can cause a wide variety of effects in the cell. Thus, the identification of AST-C receptors as GPCRs led us to hypothesize that they activate second messenger cascades and therefore that the differential expression of factors within the cascade—and downstream from the receptors—could be important in determining physiological response. This hypothesis is supported by the findings, as differential expression and GO term analysis revealed a number of transcripts associated with second messenger cascades that were either up- or downregulated with physiological response.

Among the transcripts upregulated with increasing change in contraction amplitude were a number of serine/threonine protein kinases such as Gck III ortholog, Slik, Hippo, and Happyhour. These transcripts are consistent with our hypothesis that downstream factors would be differentially expressed based on physiological response because kinases like these are some of the most important proteins associated with second messenger cascades. Kinases phosphorylate other proteins and, in doing so, can activate or inactivate their targets. Furthermore, other types of downstream factors were downregulated with increasing change in

contraction amplitude in response to AST-C. These factors include transient receptor potential proteins, or TRP channels, which have high calcium ion permeability and are regulated by lipid second messengers (Hardie, 2003). Differential expression of calcium channels is particularly interesting in this system because the cardiac ganglion functions largely through calcium currents (Ransdell et al., 2013). Identification of differentially expressed transcripts in this project is particularly useful in helping to reveal the pathways and mechanisms through which AST-C alters cardiac ganglion output and the patterning of the lobster heartbeat. Based on GO term analysis, pathways such as MAPK, JNK, and Hippo all seem to be relevant in the downstream response to AST-C receptor activation. Further experimentation looking closely at the role of specific components of these pathways will have to be performed to elucidate how these transcripts and pathways are interacting in response to perfusion of C-type allatostatin through the cardiac neuromuscular system.

Going forward, these data could be further supported through a few additional experiments. First, RT-qPCR could be performed on a second dataset of lobsters that have known physiological responses in order to confirm differential expression of select transcripts—such as AST-CR1, protein kinases like Hippo and Happyhour, and ion channels like TRP channels—based on physiological response to AST-C. Furthermore, there is the potential for physiological experiments in which the differentially expressed transcripts are pharmacologically targeted. These experiments would entail recording a lobster's natural physiological response to AST-C, and then perfusing a drug or toxin through the lobster's heart to either increase or decrease the effect of a specific protein before recording the physiological response to AST-C again. This pharmacological intervention, as well as RT-qPCR experiments, could confirm the

roles of the differentially expressed transcripts identified in this project in the cardiac neuromuscular system's response to C-type allatostatin.

Further research also needs to be conducted to investigate the potential cause of the individual variation that is observed in response to perfusion of AST-C I and III. Analysis of the Illumina RNA-Sequencing data of hypodermis and eyestalk samples will help investigate the role that the molt cycle may play in AST-C response. Our current hypothesis is that the stage of the molt cycle of the lobster determines its response to AST-C. Preliminary findings show that lobsters that responded with an increase in heartbeat amplitude to AST-C had an upregulation of RNA transcripts associated with growth, such as those associated with ribosomal structure; these findings are consistent with the responses being mapped onto a stress axis. It is possible that when lobsters have an increased amplitude response they are at a certain point in their molt cycle when growth is prioritized; however, when the process of molting causes the lobster stress, it downregulates any processes that are not necessary for survival and this is when we see a decreased amplitude response. If this hypothesis is correct and AST-C response is correlated with a lobster's molt stage, this information could further our understanding of AST-C's physiological function as well as its association with other molt-related peptides and hormones, like ecdysteroids and neuropeptide hormones (Techa and Chung, 2015; Oliphant et al., 2018). Further investigation into these questions and hypotheses will help reveal why there is such great individual variation between lobsters in addition to how that variation arises mechanistically.

In conclusion, these findings support our hypothesis of an underlying RNA expression-dependent mechanism for individual variation in cardiac neuromuscular system response to AST-C. An individual lobster's cardiac response to AST-C can be understood based on expression levels of AST-C receptor 1, protein kinases, and other factors in second messenger

cascades. These findings and future experiments building off of them will help contribute to our overall understanding of individual variation in response to peptides within a population, a biological mechanism that is relevant beyond the cardiac neuromuscular system of the American lobster.

Tables & Figures

Introduction

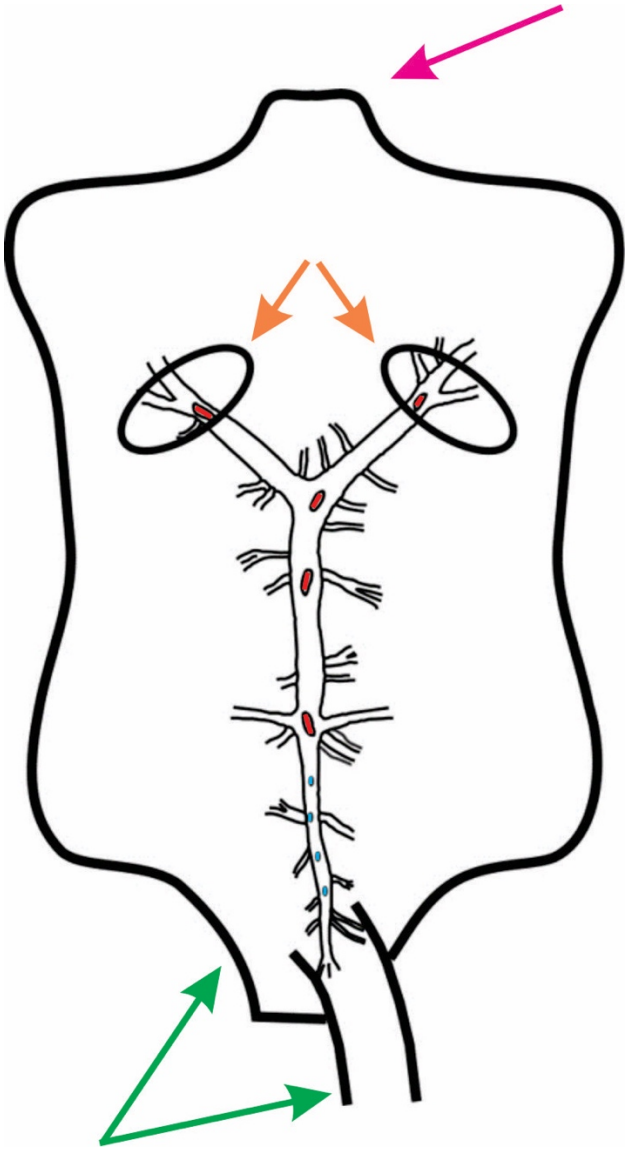

Figure 1. A schematic ventral view of the cardiac neuromuscular system of the American lobster (*Homarus americanus*). The cardiac ganglion (Y-shaped structure) is shown embedded in the dorsal wall of the heart. Within the cardiac ganglion, the nine cell bodies of the neurons that comprise it are pictured. There are five larger, anterior motor neurons (shown in red) and four smaller, posterior pacemaker neurons (shown in blue). Pictured schematically are the two posterior arteries (green arrows) and five anterior arteries (represented by the outline denoted by pink arrow) as well as the two ostia that are located in the ventral wall of the heart (orange arrows).

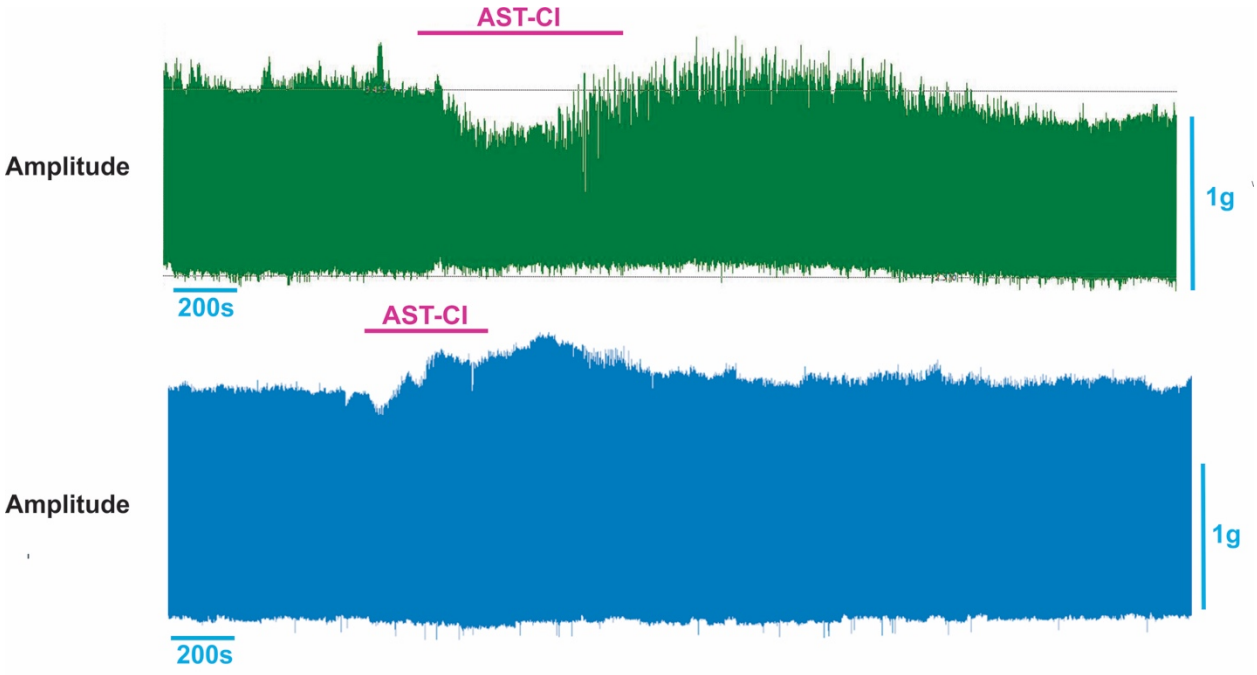

Figure 2. Sample recordings from two different lobsters showing opposite responses in change in amplitude of the heartbeat to perfusion of AST-C I. The time scale of both recordings is compressed. The top recording shows a decrease in heartbeat amplitude in response to AST-C I, while the bottom recording shows an increase in amplitude. These recordings illustrate the individual variation present in lobsters' responses to AST-C. All recordings were performed in Spike2.

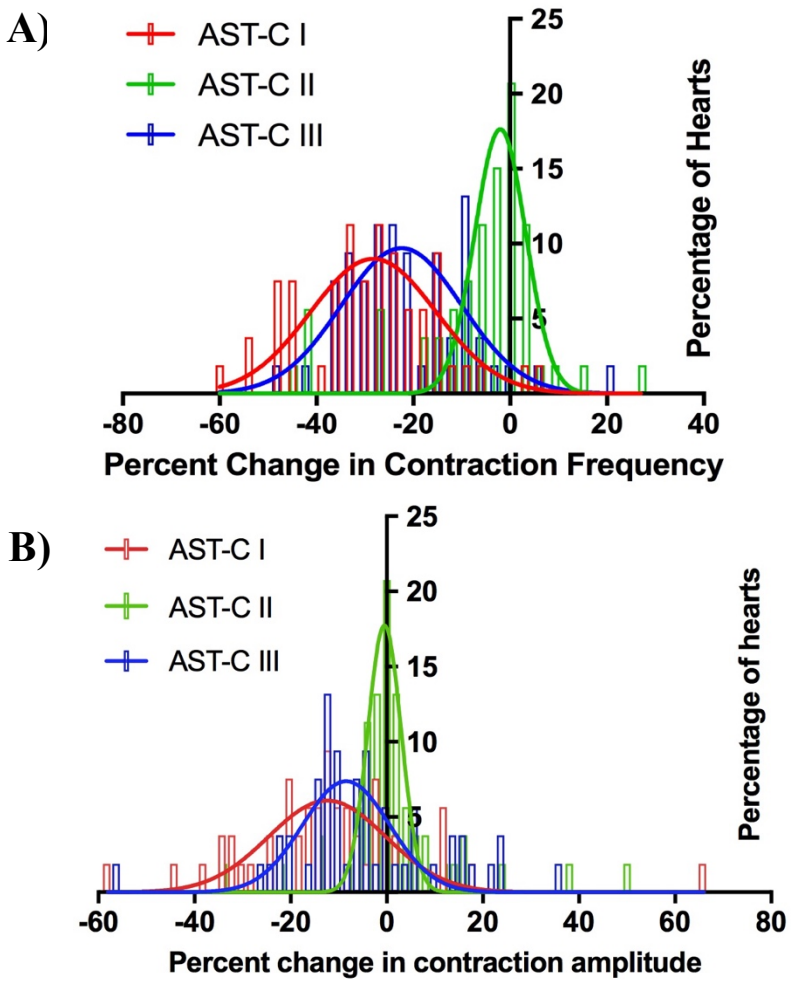

Figure 3. Adapted from Dickinson et al. (2018). Distribution of responses of the cardiac neuromuscular system to perfusion of the three endogenous C-type allatostatins (AST-C I, II, and III). (A) Percent changes in contraction frequency of the heartbeat to each AST-C isoform. (B) Percent changes in contraction amplitude of the heartbeat to each AST-C isoform. Because responses to AST-C are highly variable, the distributions of responses allow for a more comprehensive analysis. For both frequency and amplitude responses, the distributions of AST-C I and III are more similar to each other than they are to the distribution of AST-C II. Additionally, there are particularly wide distributions of responses to both AST-C I and III, showing great variation among individual lobsters.

Table 1. Sequences of the endogenous and synthetic AST-C isoforms that were used to test the effect of C-terminal amidation on the physiological response to AST-C. AST-C I and III had amidation added at the C-terminus in the synthetic isoforms (shown in red). AST-C II had its C-terminal amidation removed in the synthetic isoform. Bolded amino acids represent the conserved sequence of the peptide.

Isoform	Endogenous	Synthetic
AST-C I	pQIRYHQ**CYFNPISCF**	pQIRYHQ**CYFNPISCF**a
AST-C II	SYWKQ**CAFNAVSCF**a	SYWKQ**CAFNAVSCF**
AST-C III	GNGDGRLYWR**CYFNAVSCF**	GNGDGRLYWR**CYFNAVSCF**a

Table 2. Sequences of the endogenous and synthetic AST-C isoforms that were applied to the isolated whole heart in order to observe the effects of the neuropeptide on the contraction of the heartbeat. Bolded amino acids represent the conserved sequence of the peptide. The purple and blue amino acids are highlighted because—in the endogenous isoforms—AST-C I and III contain tyrosine (Y) and AST-C II has an alanine (A) at that position. The amino acids at these positions were changed in the synthetic isoforms in order to test the hypothesis that the presence of either tyrosine or alanine is the mechanism underlying the differences in the response distributions between AST-C II and AST-C I and III. The endogenous AST-C I was not included in the analysis of the physiological data as we did not have a synthetic AST-C I A for comparison.

Isoform	Endogenous	Synthetic
AST-C I	pQIRYHQ**C**Y**FNPISCF**	-
AST-C II	SYWKQ**C**A**FNAVSCF**a	SYWKQ**C**Y**FNAVSCF**a
AST-C III	GNGDGRLYWR**C**Y**FNAVSCF**	GNGDGRLYWR**C**A**FNAVSCF**

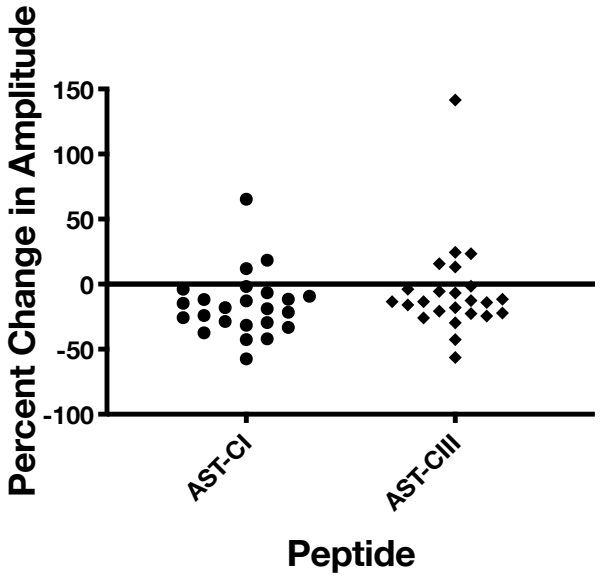

Figure 4. Responses in contraction amplitude of the heartbeat to AST-C I and III of the 24 lobsters that had the RNA of their cardiac ganglia sequenced. The percent change from baseline in contraction amplitude of the heartbeat is shown. These lobsters were chosen based on their wide range of changes in heartbeat amplitude to AST-C and the quality and quantity of RNA.

Table 3. Bioinformatic programs used for Illumina RNA-Sequencing data processing and analysis. FastQC, Trimmomatic, Kallisto, BowTie2, CD-HIT-EST, and TransDecoder were run on Bowdoin College Computing Grid (moosehead) using command line interface. JMP Version 13 was run by Joel Graber (Bioinformatics Core, Mount Desert Island Biological Laboratory, Bar Harbor, ME). DESeq2 was run in RStudio Version 1.2.1335.

Program	Function	Access URL
FastQC	Performs quality control checks on high throughput sequencing data	https://www.bioinformatics.babraham.ac.uk/projects/fastqc/
Trimmomatic	Eliminates and shortens reads based on Phred quality scores	http://www.usadellab.org/cms/?page=trimmomatic
Kallisto	Uses "pseudoalignment" to map sample reads to a target transcriptome and determine abundances of transcripts within a sample	https://pachterlab.github.io/kallisto/about
BowTie2	Aligns sequencing reads to references (transcriptome) to quantify the amount of each transcript in a sample	http://bowtie-bio.sourceforge.net/bowtie2/index.shtml
CD-HIT-EST	Clusters sequences based on a similarity threshold in order to reduce the number of individual hits	http://weizhongli-lab.org/cd-hit/
TransDecoder	Identifies sequences of RNA that are likely to be coding regions	https://github.com/TransDecoder/TransDecoder/wiki
JMP	Statistical software used to perform principal component analysis	https://www.jmp.com/en_us/home.html
DESeq2	Performs differential expression analysis to determine if variance of expression between samples is related to the variable of interest	https://bioconductor.org/packages/release/bioc/html/DESeq2.html
Gene Ontology	Outputs GO terms of biological processes associated with genes	http://geneontology.org/

Results

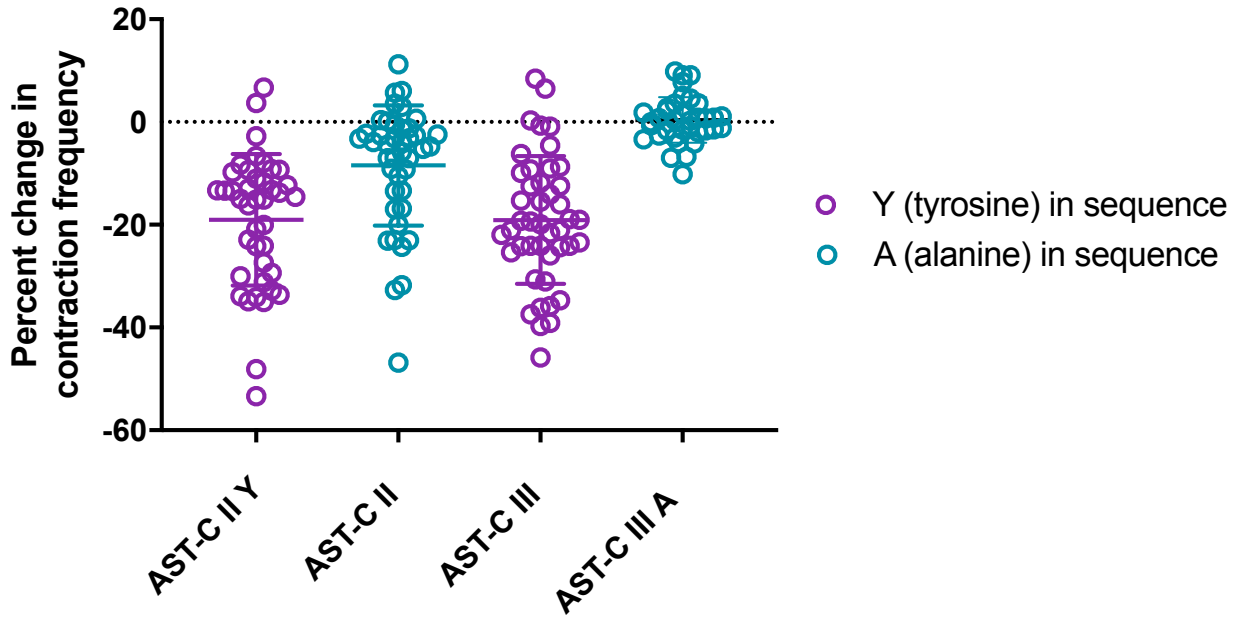

Figure 5. Percent changes in frequency of lobsters (n=44) to two endogenous (AST-C II and III) and two synthetic isoforms (AST-C II Y and III A). Each lobster had its response characterized to each isoform; the same 44 lobsters comprise the data for each isoform. A one-way ANOVA with Tukey's multiple comparisons test was performed to analyze differences in mean percent change in frequency between isoforms and Kolmogorov-Smirnov tests were performed to analyze differences in shapes of the distributions. Statistical test results are shown in Table 4.

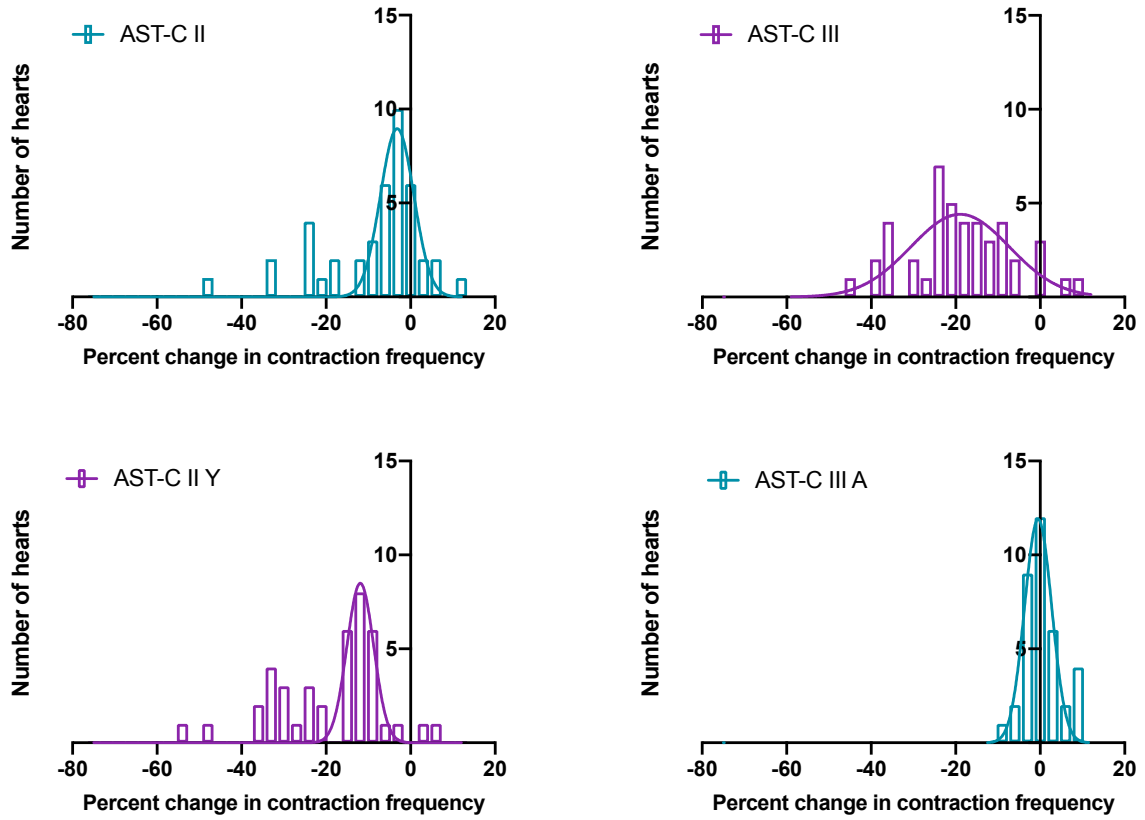

Figure 6. Distributions of frequency responses of the cardiac neuromuscular system of 44 lobsters to endogenous and synthetic AST-C isoforms. Isoforms shown in purple have a tyrosine in their conserved sequences, while isoforms in blue have an alanine in their conserved sequences. Note that the two isoforms that contain tyrosine (AST-C III and II Y) have wider distributions centered further below zero than the two that contain alanine (AST-C II and III A). Curves represent non-linear fits of the distribution.

Table 4. Results of statistical tests of the percent change in frequency in response to AST-C II, II Y, III, and III A isoforms. Blue isoforms have an alanine in their conserved sequence, while purple isoforms have a tyrosine in the same spot of the conserved sequence. A one-way ANOVA followed by Tukey's multiple comparisons tests was performed to analyze mean responses (α = 0.05). Kolmogorov-Smirnov (K-S) tests were performed to analyze distribution shapes (α = 0.008, Bonferroni's correction). The means and distribution shapes are significantly different from each other in every comparison except between the two isoforms with tyrosine in their sequences (AST-C II Y and III).

Frequency Comparison	Difference in Means? (Tukey's p-value)	Difference in Distributions? (K-S Test p-value)
AST-C II Y vs AST-C II	Yes ($p = 0.0001$)	Yes ($p < 0.0001$)
AST-C II Y vs AST-C III	No ($p > 0.9999$)	No ($p = 0.2555$)
AST-C II Y vs AST-C III A	Yes ($p < 0.0001$)	Yes ($p < 0.0001$)
AST-C II vs AST-C III	Yes ($p < 0.0001$)	Yes ($p < 0.0001$)
AST-C II vs AST-C III A	Yes ($p = 0.0031$)	Yes ($p < 0.0001$)
AST-C III vs AST-C III A	Yes ($p < 0.0001$)	Yes ($p < 0.0001$)

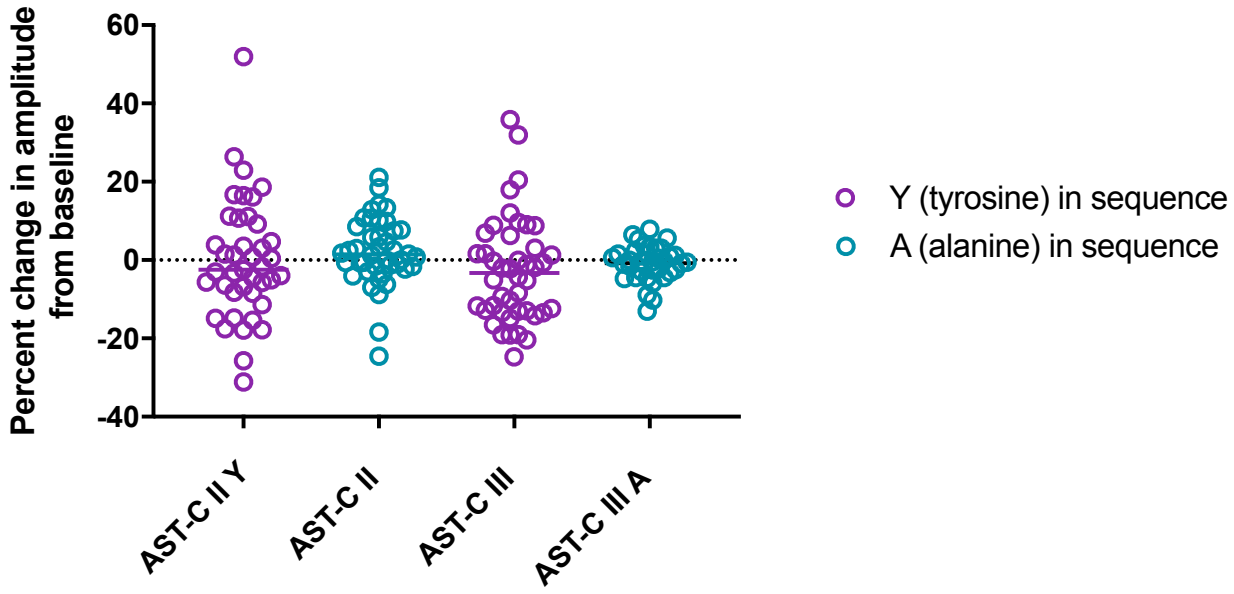

Figure 7. Percent changes in amplitude of lobsters (n=44) to two endogenous (AST-C II and III) and two synthetic isoforms (AST-C II Y and III A). Each lobster had its response characterized to each isoform; the same 44 lobsters comprise the data for each isoform. A one-way ANOVA with Tukey's multiple comparisons test was performed to analyze differences in mean percent change in amplitude between isoforms and Kolmogorov-Smirnov tests were performed to analyze differences in shapes of the distributions. Statistical test results are shown in Table 5.

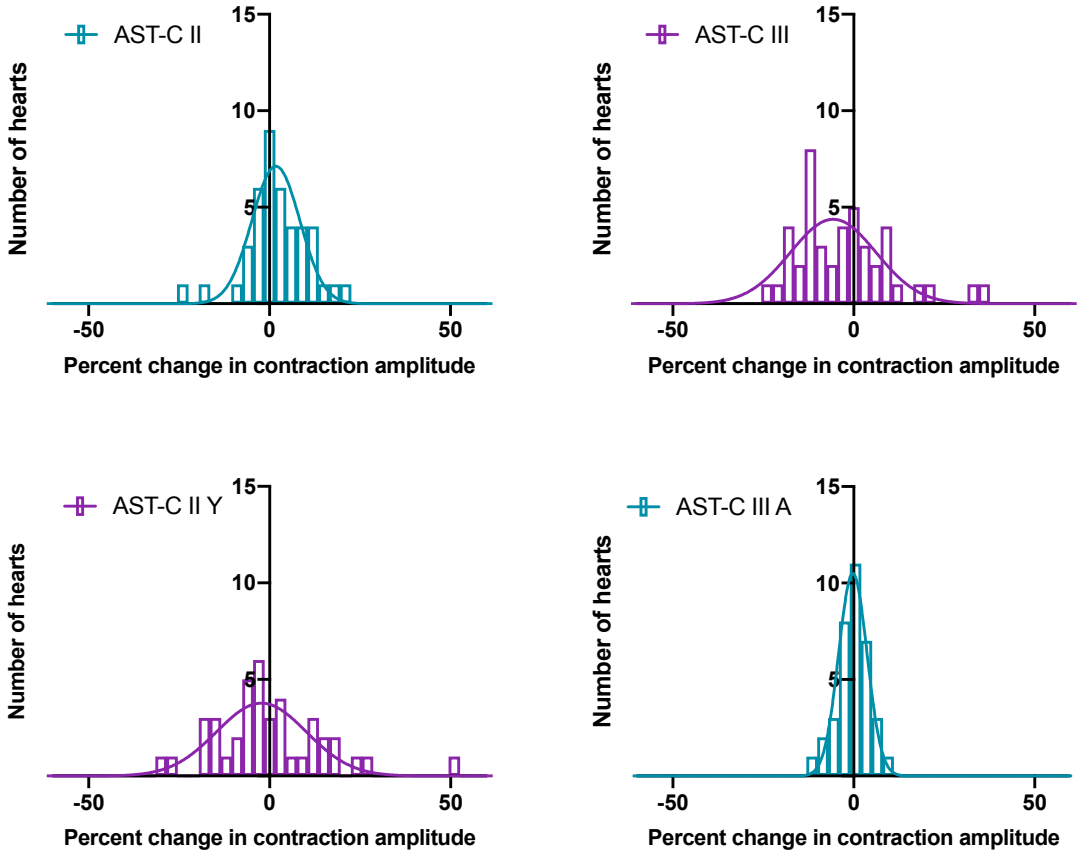

Figure 8. Distributions of amplitude responses of the cardiac neuromuscular system of 44 lobsters to endogenous and synthetic AST-C isoforms. Isoforms shown in purple have a tyrosine in their conserved sequences, while isoforms in blue have an alanine in their conserved sequences. Note that the two isoforms that contain tyrosine (AST-C III and II Y) have wider distributions than the two that contain alanine (AST-C II and III A). Curves represent non-linear fits of the distribution.

Table 5. Results of statistical tests of the percent change in amplitude in response to AST-C II, II Y, III, and III A isoforms. Blue isoforms have an alanine in their conserved sequence, while purple isoforms have a tyrosine in the same spot of the conserved sequence. A one-way ANOVA followed by Tukey's multiple comparisons tests was performed to analyze means ($\alpha = 0.05$). Kolmogorov-Smirnov (K-S) tests were performed to analyze distribution shapes ($\alpha = 0.008$, Bonferroni's correction). The only significant difference in amplitude response is between the means of the two endogenous isoforms (AST-C II and III).

Amplitude Comparison	Difference in Means? (ANOVA p-value)	Difference in Distributions? (K-S Test p-value)
AST-C II Y vs AST-C II	No ($p = 0.8296$)	No ($p = 0.0496$)
AST-C II Y vs AST-C III	No ($p = 0.6733$)	No ($p = 0.4305$)
AST-C II Y vs AST-C III A	No ($p = 0.9924$)	No ($p = 0.1009$)
AST-C II vs AST-C III	No ($p = 0.1920$)	Yes ($p = 0.0073$)
AST-C II vs AST-C III A	No ($p = 0.6876$)	No ($p = 0.1004$)
AST-C III vs AST-C III A	No ($p = 0.8521$)	No ($p = 0.0099$)

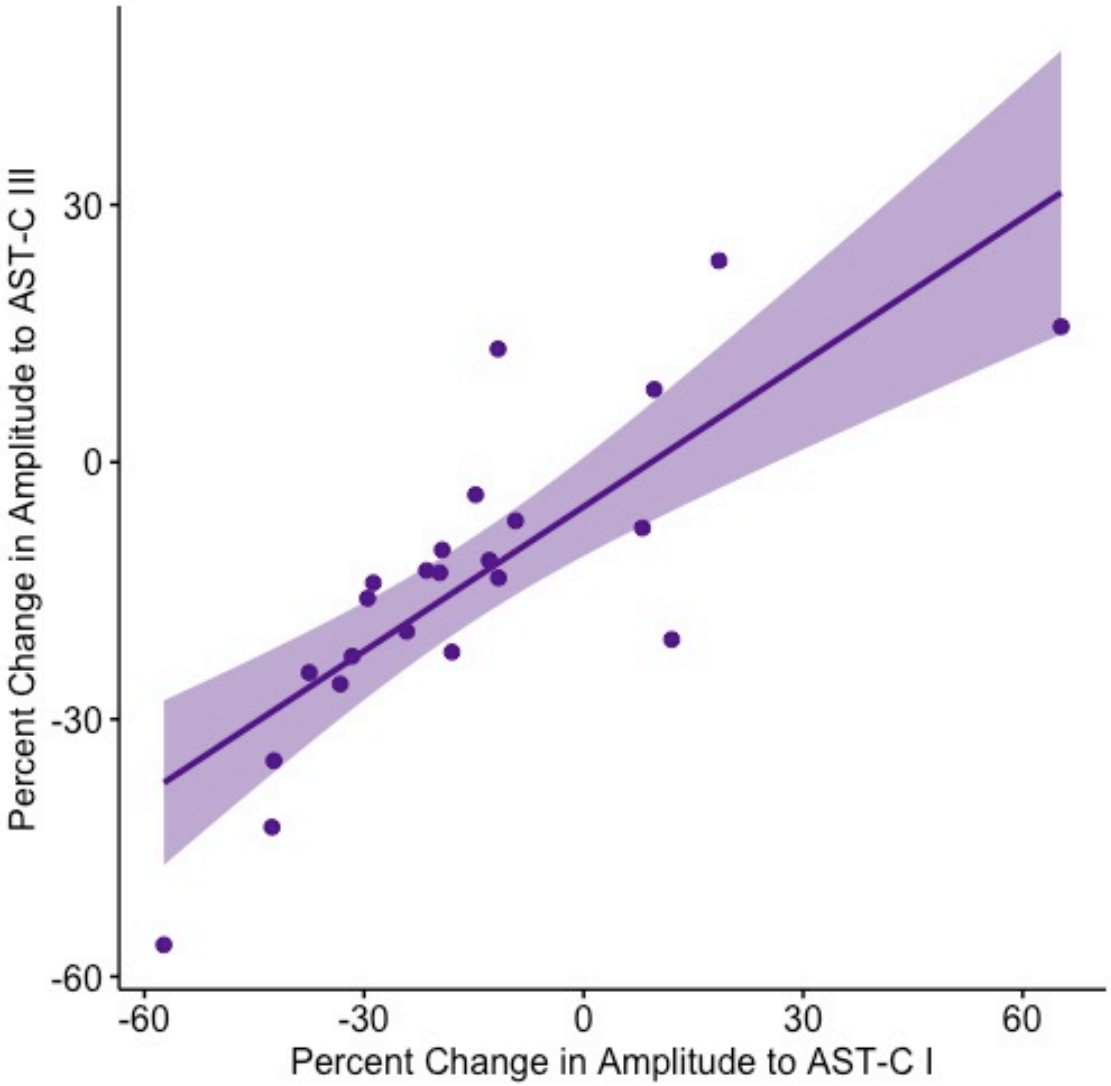

Figure 9. Spearman correlation between the percent changes in amplitude to AST-C I and AST-C III of the dataset of lobsters that had their cardiac ganglion RNA sequenced. One outlier was omitted using the GraphPad Prism ROUT Method (n=23). The correlation has a Spearman coefficient (R) of 0.83 and a p-value < 0.0001, suggesting a strong positive correlation between a lobster's cardiac responses to AST-C I and AST-C III.

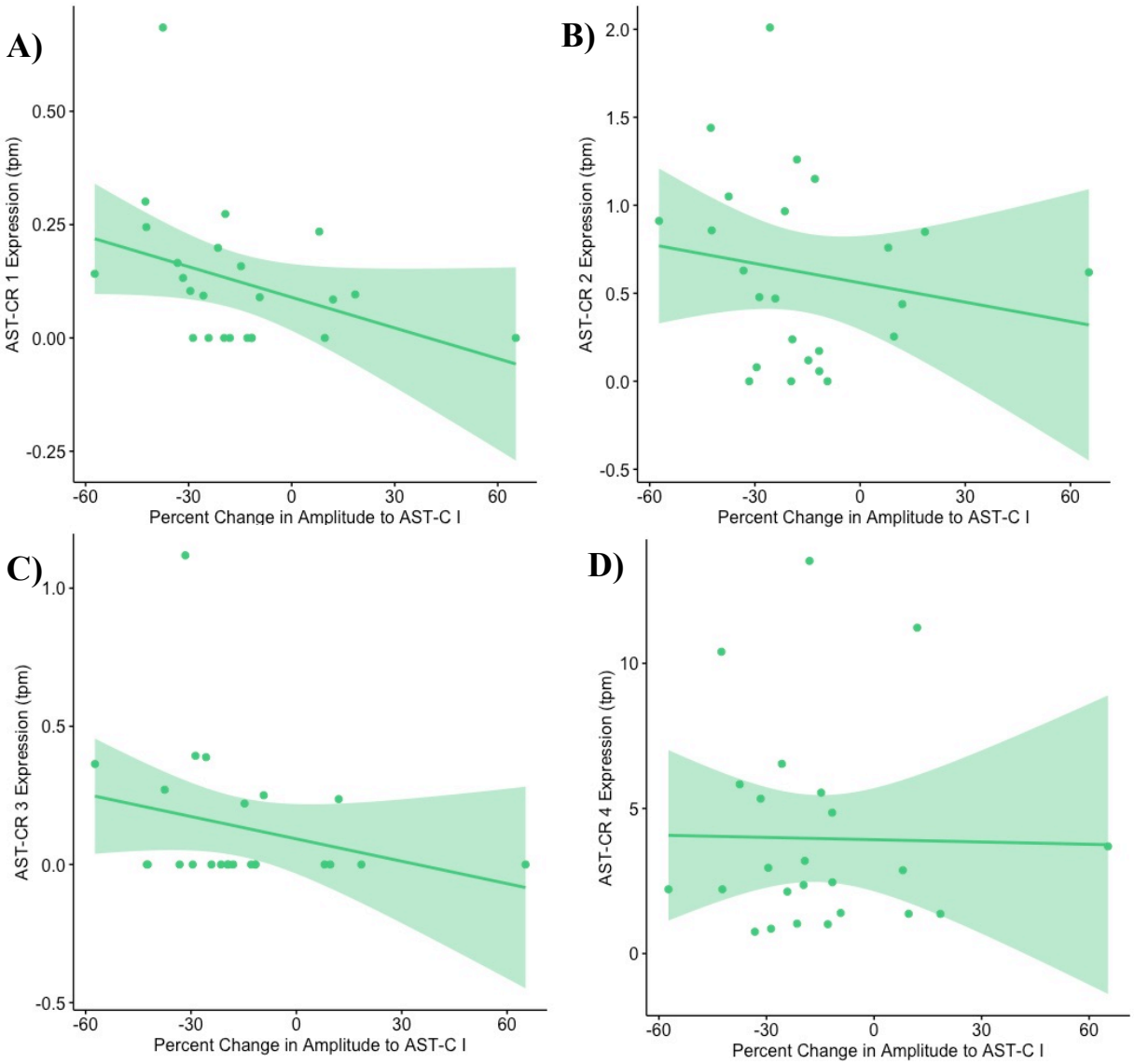

Figure 10. Spearman correlations of the percent change in amplitude to AST-C I and the expression of each AST-C receptor (n=23 lobsters). (A) There was a significant negative correlation between the expression of AST-C receptor 1 and AST-C I physiological response (R= -0.5, p = 0.012). (B-D) The correlations between AST-C receptors 2-4 and percent change in amplitude to AST-C I were not significant (AST-CR 2: R= -0.27, p=0.2; AST-CR 3: R=-0.28, p=0.18; AST-CR 4: R=-0.021, p=0.92).

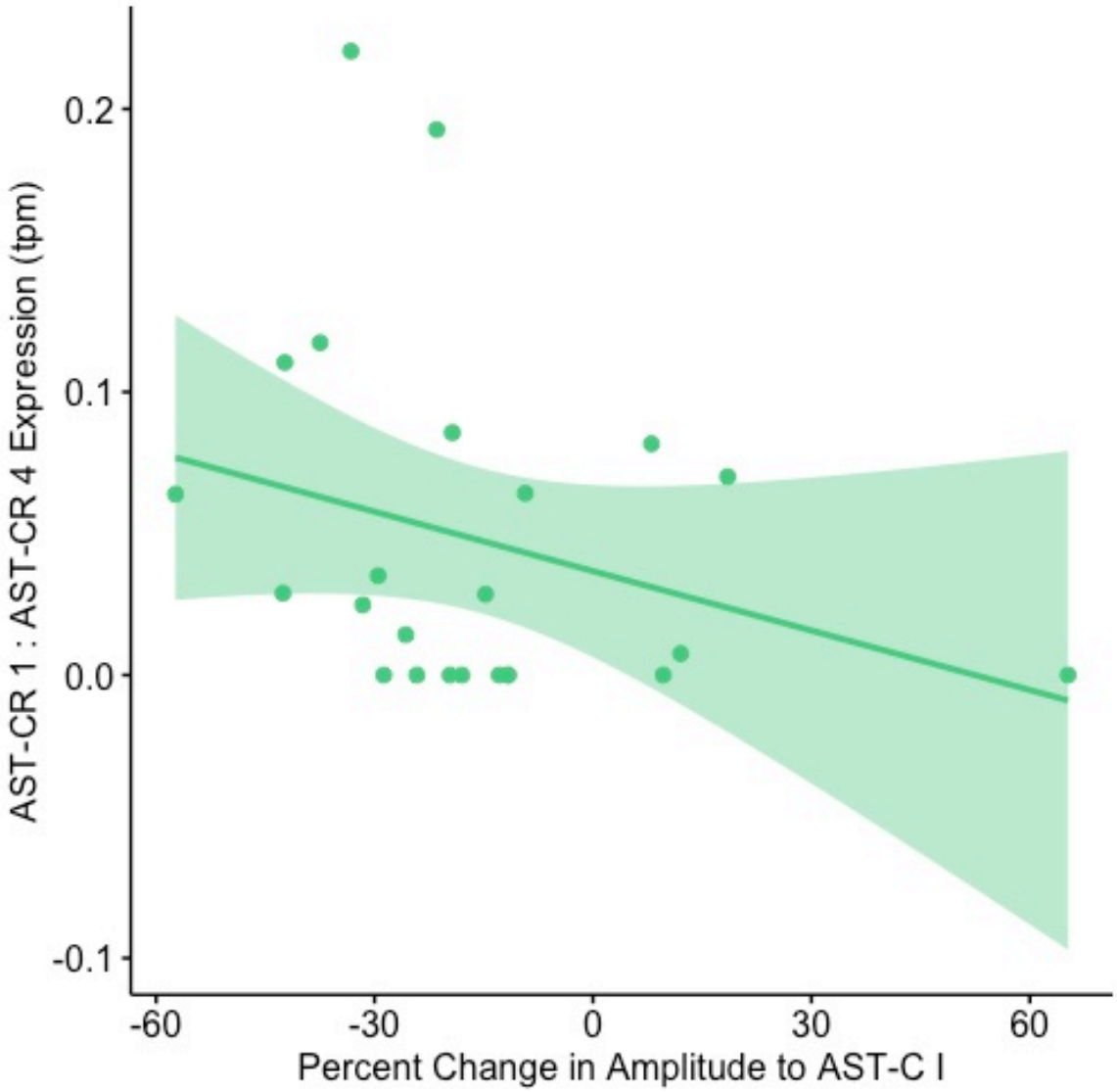

Figure 11. Spearman correlation of the response in amplitude to AST-C I and the ratio of expression of AST-C receptors I and IV (n=23 lobsters). These data show a slight negative correlation trending towards significance (R= -0.37, p= 0.075). The ratios of all other receptors to each other and to total receptor expression were analyzed via Spearman correlation, but all other combinations had weaker or less significant correlations than this one.

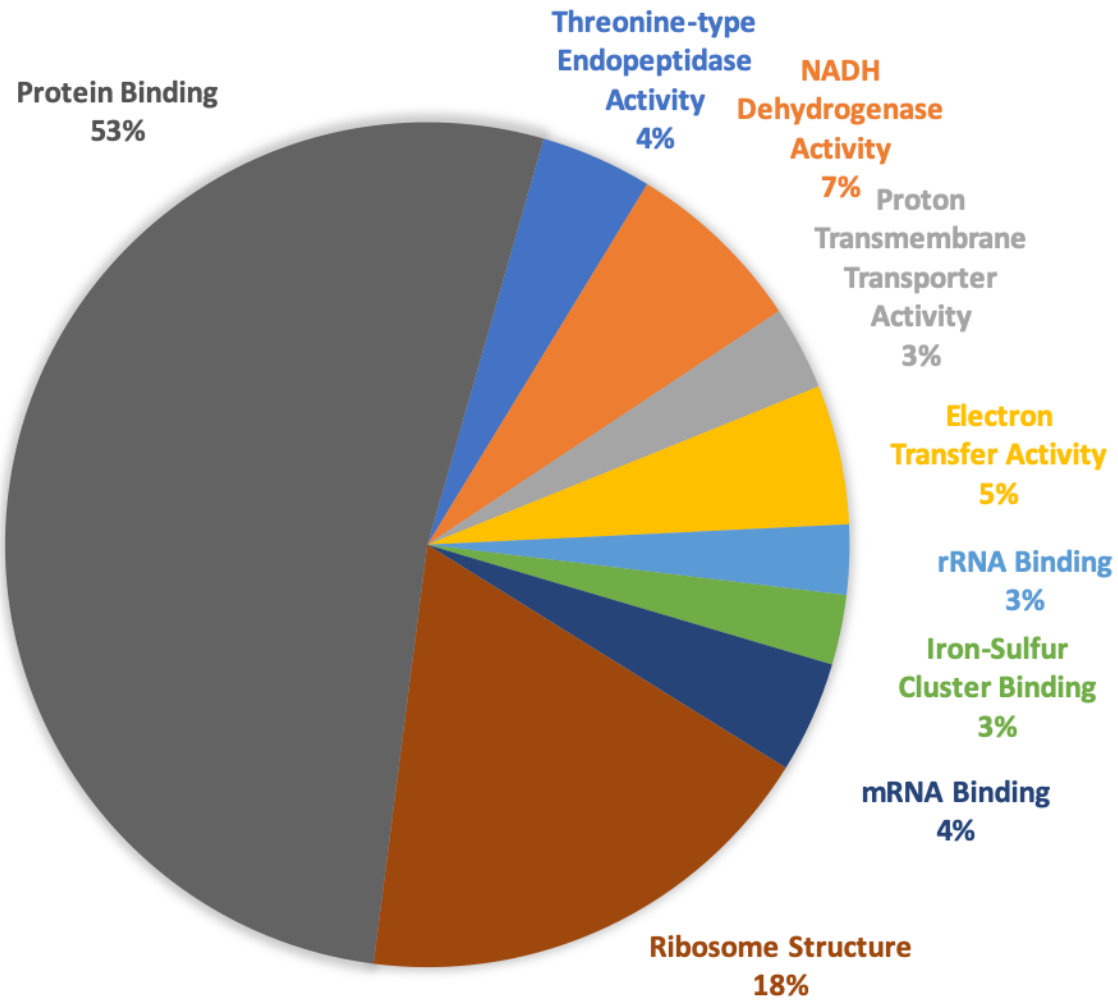

Figure 12. Distribution of Gene Ontology (GO) terms of the molecular functions of genes positively correlated with AST-C I physiological response. These genes (n=128) were identified through principal component analysis. GO terms were obtained from geneontology.org.

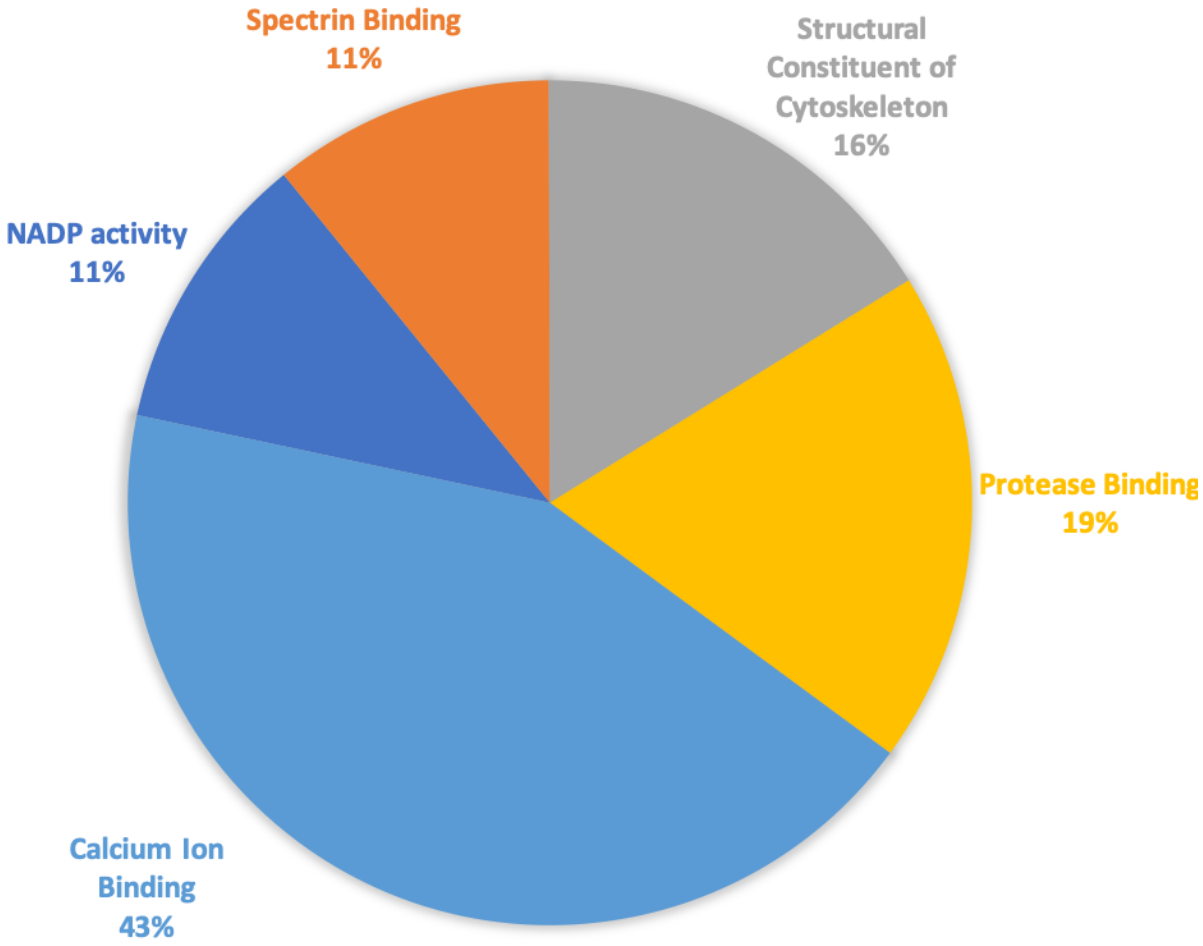

Figure 13. Distribution of GO terms of the molecular functions of genes negatively correlated with AST-C I physiological response. These genes (n=132) were identified through principal component analysis. GO terms were obtained from geneontology.org.

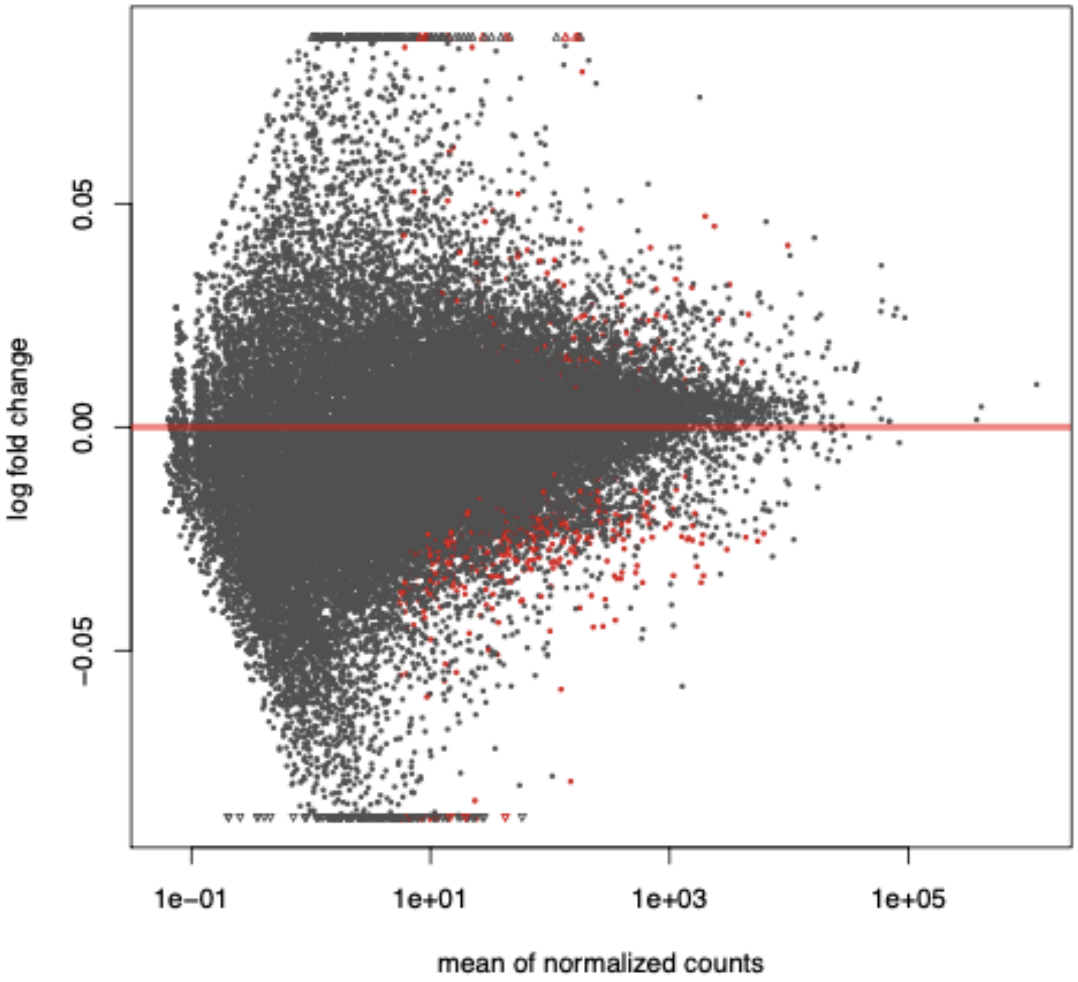

Figure 14. DESeq2 plot of the log fold change and mean of normalized counts for each transcript identified in the samples. Each dot represents a transcript; red dots are those identified as being significantly differentially expressed by DESeq2. 615 total transcripts were identified as being differentially expressed based on AST-C I physiological response (adjusted p-value < 0.10). Transcripts above the red line are those that are upregulated (140 significant transcripts) with increasing percent change in amplitude to AST-C I, while ones below the red line are downregulated (475 significant transcripts) with increasing percent change in amplitude to AST-C I. One sample has been eliminated from this analysis because it was identified as an outlier that was dominating the second principal component.

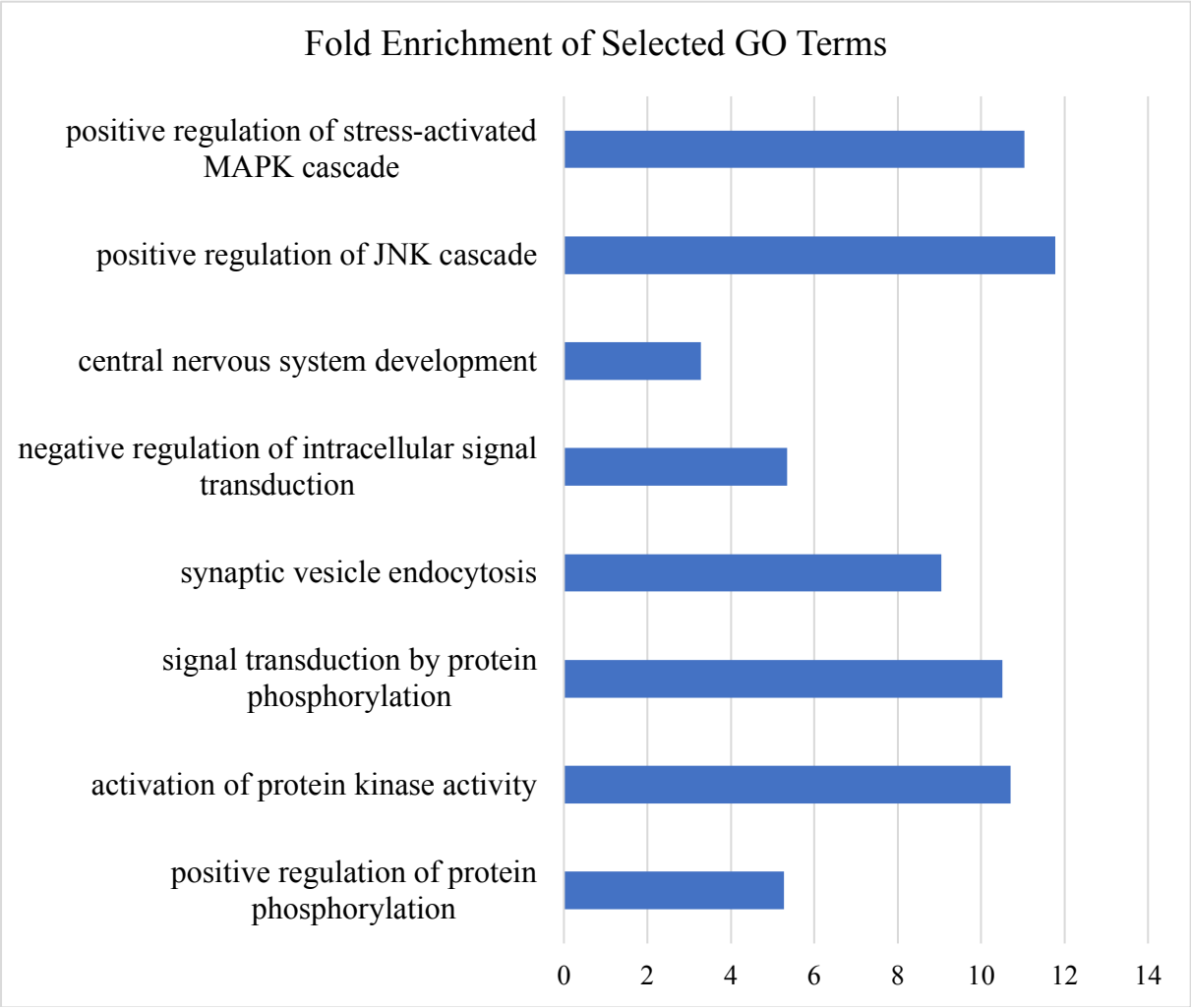

Figure 15. Fold enrichment values of selected relevant GO terms from Gene Ontology analysis of the set of differentially expressed transcripts that were positively correlated with increasing change in contraction amplitude in response to AST-C I and matched to FlyBase. 389 FlyBase-matched transcripts were queried into Gene Ontology. These GO terms were pulled out of the full set (available in Appendix B) due to their relevance to neural processes and second messenger cascades believed to be associated with the downstream effects of the AST-C receptors.

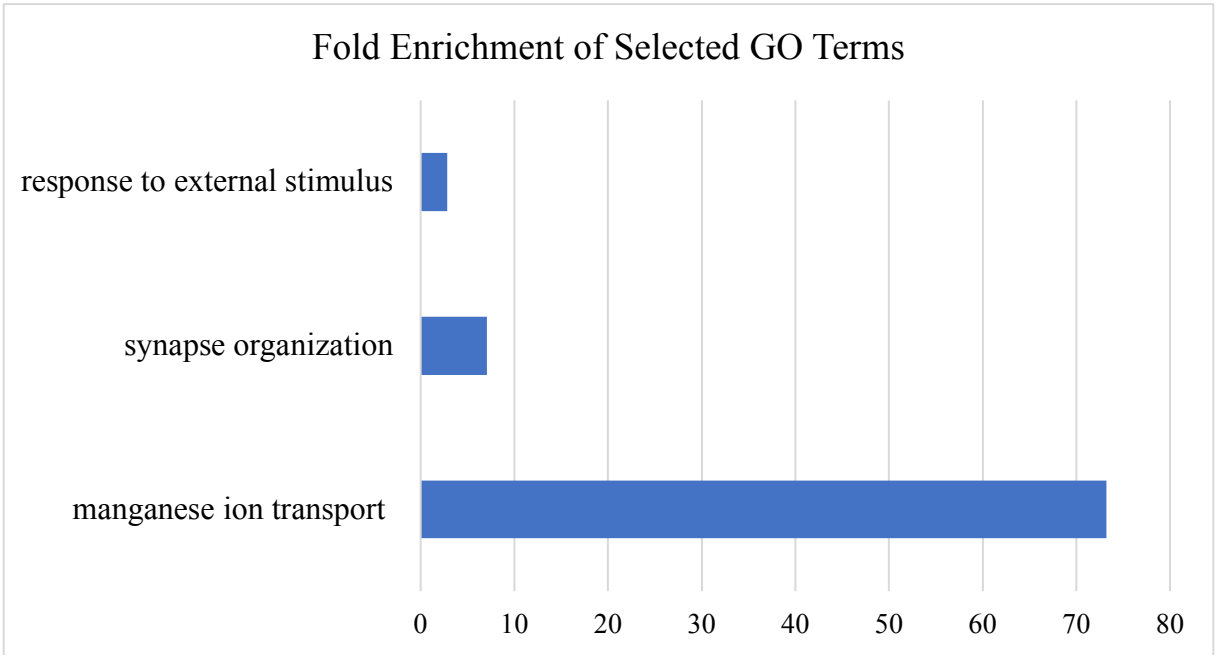

Figure 16. Fold enrichment values of selected relevant GO terms from Gene Ontology analysis of the set of differentially expressed transcripts that were negatively correlated with increasing change in contraction amplitude in response to AST-C I and matched to FlyBase. 361 FlyBase-matched transcripts were queried into Gene Ontolgy. These GO terms were pulled out of the full set (available in Appendix B) due to their relevance to neural processes and second messenger cascades believed to be associated with the downstream effects of the AST-C receptors.

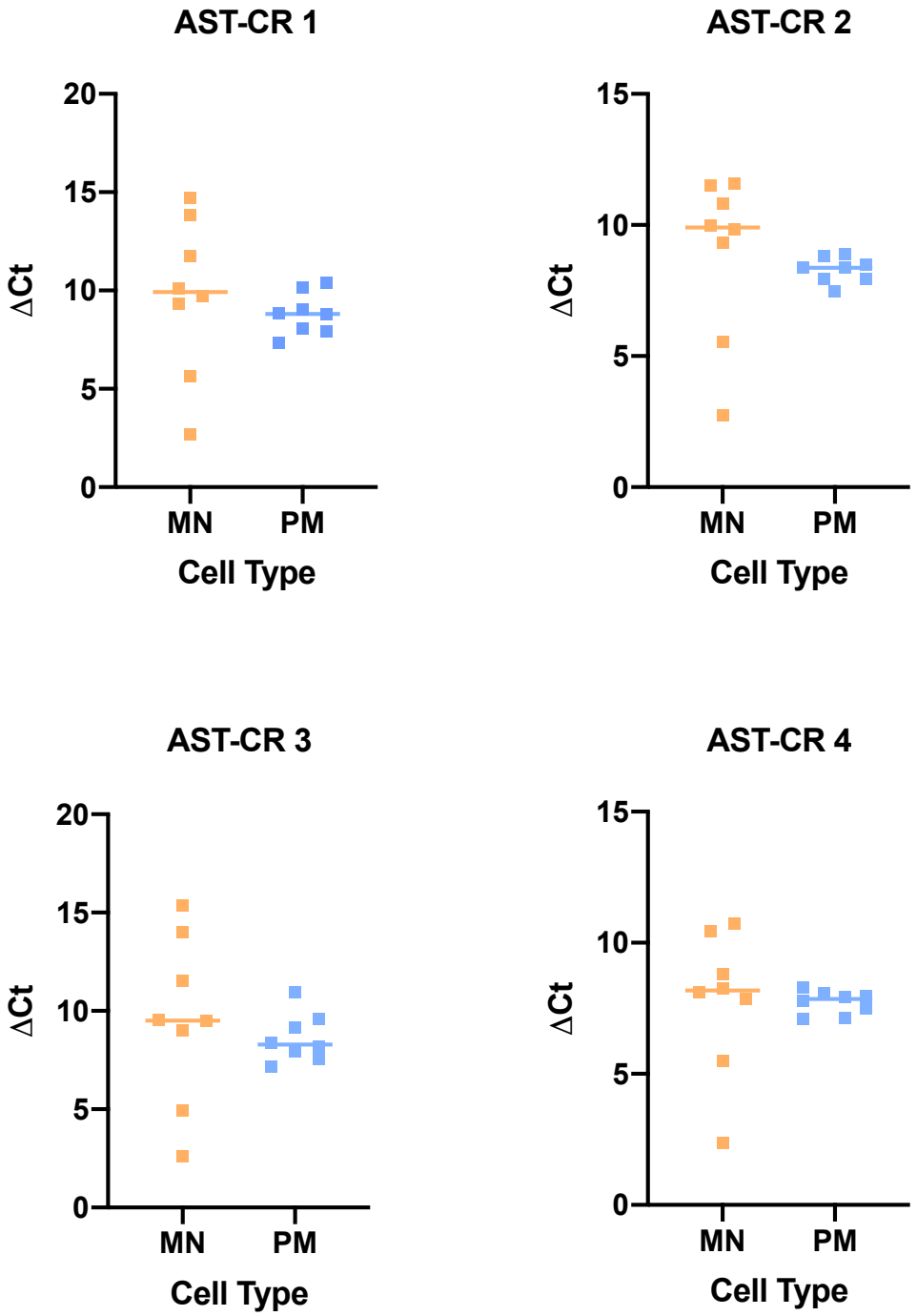

Figure 17. Expression of the four AST-C receptors measured by RT-qPCR and separated by cardiac ganglion cell type (MN: motor neurons; PM: pacemaker) (n=8 lobsters). The average expression between cell types did not differ significantly for any of the receptor types (Paired T-tests, α=0.05, AST-CR 1: $p = 0.6107$, AST-CR 2: $p = 0.5968$, AST-CR 3: $p = 0.6340$, AST-CR 4: $p = 0.9745$). However, the variance of receptor expression levels differed significantly between cell types for all four receptors (F-tests for variance, α=0.05, AST-CR 1: $p = 0.0023$, AST-CR 2: $p < 0.0001$, AST-CR 3: $p = 0.0042$, AST-CR 4: $p < 0.0001$).

Literature Cited

Ackers GK, Smith FR (1985) Effects of Site-Specific Amino Acid Modification on Protein Interactions and Biological Function. Annual Review of Biochemistry 54:597-629.

Betts MJ, Russell RB (2003) Amino Acid Properties and Consequences of Substitutions. In: Bioinformatics for Geneticists (Barnes MR, Gray IC, eds). West Sussex, England: John Wiley & Sons Ltd.

Bhattacharya A, Gu GG, Singh S (1999) Modulation of dihydropyridine-sensitive calcium channels in Drosophila by a cAMP-mediated pathway. Journal of neurobiology 39:491-500.

Cerveau N, Jackson DJ (2016) Combining independent de novo assemblies optimizes the coding transcriptome for nonconventional model eukaryotic organisms. BMC Bioinformatics 17:525.

Chang ES (1995) Physiological and biochemical changes during the molt cycle in decapod crustaceans: an overview. Journal of Experimental Marine Biology and Ecology 193:1-14.

Chang ES, Mykles DL (2011) Regulation of crustacean molting: A review and our perspectives. General and Comparative Endocrinology 172:323-330.

Christie AE, Chi M, Lameyer TJ, Pascual MG, Shea DN, Stanhope ME, Schulz DJ, Dickinson PS (2015) Neuropeptidergic Signaling in the American Lobster Homarus americanus: New Insights from High-Throughput Nucleotide Sequencing. PloS one 10:e0145964-e0145964.

Christie AE, Roncalli V, Cieslak MC, Pascual MG, Yu A, Lameyer TJ, Stanhope ME, Dickinson PS (2017) Prediction of a neuropeptidome for the eyestalk ganglia of the lobster Homarus americanus using a tissue-specific de novo assembled transcriptome. General and Comparative Endocrinology 243:96-119.

Christie AE, Yu A, Roncalli V, Pascual MG, Cieslak MC, Warner AN, Lameyer TJ, Stanhope ME, Dickinson PS, Hull JJ (2018a) Molecular evidence for an intrinsic circadian pacemaker in the cardiac ganglion of the American lobster, Homarus americanus - Is diel cycling of heartbeat frequency controlled by a peripheral clock system ? Marine Genomics 41:19-30.

Christie AE, Yu A, Pascual MG, Roncalli V, Cieslak MC, Warner AN, Lameyer TJ, Stanhope ME, Dickinson PS, Joe Hull J (2018b) Circadian signaling in Homarus americanus: Region-specific de novo assembled transcriptomes show that both the brain and eyestalk ganglia possess the molecular components of a putative clock system. Marine Genomics 40:25-44.

Cooke IM (2002) Reliable, responsive pacemaking and pattern generation with minimal cell numbers: the crustacean cardiac ganglion. Biol Bull 202:108-136.

Corl AB, Berger KH, Ophir-Shohat G, Gesch J, Simms JA, Bartlett SE, Heberlein U (2009) Happyhour, a Ste20 Family Kinase, Implicates EGFR Signaling in Ethanol-Induced Behaviors. Cell 137:949-960.

Deng C, He X, Hsueh AJW (2013) A Single-Nucleotide Polymorphism of Human Neuropeptide S Gene Originated from Europe Shows Decreased Bioactivity. PLoS One 8.

Dickinson PS (1995) The Contributions of Motor Neuronal and Muscle Modulation to Behavioral Flexibility in the Stomatogastric System1. Integrative and Comparative Biology 35:548-555.

Dickinson PS (2006) Neuromodulation of central pattern generators in invertebrates and vertebrates. Current Opinion in Neurobiology 16:604-614.
Dickinson PS, Wiwatpanit T, Gabranski ER, Ackerman RJ, Stevens JS, Cashman CR, Stemmler EA, Christie AE (2009) Identification of SYWKQCAFNAVSCFamide: a broadly conserved crustacean C-type allatostatin-like peptide with both neuromodulatory and cardioactive properties. Journal of Experimental Biology 212:1140.
Dickinson PS, Armstrong MK, Dickinson ES, Fernandez R, Miller A, Pong S, Powers B, Pupo Wiss A, Stanhope ME, Walsh PJ, Wiwatpanit T, Christie AE (2018) Three members of a peptide family are differentially distributed and elicit differential state-dependent responses in a pattern generator-effector system. J Neurophysiol.
Duve H, Johnsen AH, Maestro J-L, Scott AG, Jaros PP, Thorpe A (1997) Isolation and identification of multiple neuropeptides of the allatosatatin superfamily in the shore crab Carcinus maenas. European Journal of Biochemistry 250:727-734.
Ferris J, Ge H, Liu L, Roman G (2006) G(o) signaling is required for Drosophila associative learning. Nature neuroscience 9:1036-1040.
Garcia VJ, Daur N, Temporal S, Schulz DJ, Bucher D (2015) Neuropeptide Receptor Transcript Expression Levels and Magnitude of Ionic Current Responses Show Cell Type-Specific Differences in a Small Motor Circuit. The Journal of Neuroscience 35:6786.
Getting PA (1989) Emerging Principles Governing the Operation of Neural Networks. Annual Review of Neuroscience 12:185-204.
Hardie RC (2003) Regulation of TRP Channels via Lipid Second Messengers. Annual Review of Physiology 65:735-759.
Hardie RC, Minke B (1992) The trp gene is essential for a light-activated Ca2+ channel in Drosophila photoreceptors. Neuron 8:643-651.
Kreienkamp H-J, Larusson HJ, Witte I, Roeder T, Birgül N, Hönck H-H, Harder S, Ellinghausen G, Buck F, Richter D (2002) Functional Annotation of Two Orphan G-protein-coupled Receptors, Drostar1 and -2, from Drosophila melanogaster and Their Ligands by Reverse Pharmacology. Journal of Biological Chemistry 277:39937-39943.
Kuramoto T, Yamagishi H (1990) Physiological Anatomy, Burst Formation, and Burst Frequency of the Cardiac Ganglion of Crustaceans. Physiological Zoology 63:102-116.
Lee JH, Budanov AV, Park EJ, Birse R, Kim TE, Perkins GA, Ocorr K, Ellisman MH, Bodmer R, Bier E, Karin M (2010) Sestrin as a feedback inhibitor of TOR that prevents age-related pathologies. Science (New York, NY) 327:1223-1228.
Mackenzie ES (2019) Mechanisms underlying variable responses to isoforms of the neuropeptide C-type allatostatin (AST-C) in the cardiac neuromuscular system of the American lobster, *Homarus americanus*. In: Neuroscience. Brunswick, ME: Bowdoin College.
Mahadevan A, Lappé J, Rhyne RT, Cruz-Bermúdez ND, Marder E, Goy MF (2004) Nitric Oxide Inhibits the Rate and Strength of Cardiac Contractions in the Lobster *Homarus americanus* by Acting on the Cardiac Ganglion. The Journal of Neuroscience 24:2813.
Marder E, Bucher D (2001) Central pattern generators and the control of rhythmic movements. Current Biology 11:R986-R996.
Mazarguil H, Gouardères C, Tafani J-AM, Marcus D, Kotani M, Mollereau C, Roumy M, Zajac J-M (2001) Structure-activity relationships of neuropeptide FF: role of C-terminal regions. Peptides 22:1471-1478.

Minke B (2010) The history of the Drosophila TRP channel: the birth of a new channel superfamily. Journal of neurogenetics 24:216-233.
Oleisky ER, Stanhope ME, Hull JJ, Christie AE, Dickinson PS (2020) Differential neuropeptide modulation of premotor and motor neurons in the lobster cardiac ganglion underlies changes in patterned neuronal output. Manuscript submitted for publication.
Oliphant A, Alexander JL, Swain MT, Webster SG, Wilcockson DC (2018) Transcriptomic analysis of crustacean neuropeptide signaling during the moult cycle in the green shore crab, Carcinus maenas. In: BMC genomics, p 711.
Ransdell JL, Temporal S, West NL, Leyrer ML, Schulz DJ (2013) Characterization of inward currents and channels underlying burst activity in motoneurons of crab cardiac ganglion. Journal of Neurophysiology 110:42-54.
Rolph MA (2019) Mechanisms underlying variable responses to isoforms of the neuropeptide C-type allatostatin (AST-C) in the American lobster, *Homarus americanus*. In: Biology. Brunswick, ME: Bowdoin College.
Stanhope M (2018) Mature and partially processed forms of a neuromodulator, myosuppressin, have differential bioactivity in the cardiac neuromuscular system of the American lobster, *Homarus americanus*. In: Neuroscience. Brunswick, ME: Bowdoin College.
Stay B, Tobe SS (2006) The Role of Allatostatins in Juvenile Hormone Synthesis in Insects and Crustaceans. Annual Review of Entomology 52:277-299.
Techa S, Chung JS (2015) Ecdysteroids Regulate the Levels of Molt-Inhibiting Hormone (MIH) Expression in the Blue Crab, Callinectes sapidus. PLOS ONE 10:e0117278.
Terwilliger NB, Dangott L, Ryan M (1999) Cryptocyanin, a crustacean molting protein: evolutionary link with arthropod hemocyanins and insect hexamerins. Proceedings of the National Academy of Sciences of the United States of America 96:2013-2018.
Tom M, Manfrin C, Chung SJ, Sagi A, Gerdol M, De Moro G, Pallavicini A, Giulianini PG (2014) Expression of cytoskeletal and molt-related genes is temporally scheduled in the hypodermis of the crayfish Procambarus clarkii during premolt. The Journal of Experimental Biology 217:4193.
Veenstra JA (2009) Allatostatin C and its paralog allatostatin double C: The arthropod somatostatins. Insect Biochemistry and Molecular Biology 39:161-170.
Walsh P (2017) Characterization of the receptors associated with the differing responses to the neuropeptide, AST-C, by the cardiac ganglion of the American lobster, *Homarus americanus*. In: Biochemistry. Brunswick, ME: Bowdoin College.
Wiwatpanit T, Powers B, Dickinson PS (2012) Inter-animal variability in the effects of C-type allatostatin on the cardiac neuromuscular system in the lobster Homarus americanus. The Journal of experimental biology 215:2308-2318.
Yazawa T, Wilkens JL, Cavey MJ, ter Keurs HEDJ, Cavey MJ (1999) Structure and contractile properties of the ostial muscle (musculus orbicularis ostii) in the heart of the American lobster. Journal of Comparative Physiology B 169:529-537.

Appendix A: Differentially Expressed Transcripts Matched to FlyBase

Upregulated with increasing change in contraction amplitude in response to AST-C I:

Gene Name	FlyBase ID
lqf-PI	FBgn0028582
dnc-PC	FBgn0000479
IP3K2-PB	FBgn0283680
Arf79F-PF	FBgn0010348
pnut-PA	FBgn0013726
glu-PA	FBgn0015391
Snp-PD	FBgn0265192
crn-PA	FBgn0000377
Usp2-PI	FBgn0031187
CG5171-PA	FBgn0031907
Arpc2-PB	FBgn0032859
Sur-8-PF	FBgn0038504
Dab-PD	FBgn0000414
CG6841-PA	FBgn0036828
Doa-PL	FBgn0265998
CG9297-PA	FBgn0038181
CG1129-PE	FBgn0037279
flr-PB	FBgn0260049
Dab-PI	FBgn0000414
CG4768-PA	FBgn0030790
Zasp52-PI	FBgn0265991
Inx3-PC	FBgn0265274
mthl10-PF	FBgn0035132
Parp-PB	FBgn0010247
Vps37B-PA	FBgn0037299
Gat-PA	FBgn0039915
CG17765-PA	FBgn0033529
Slc45-1-PB	FBgn0035968
DPCoAC-PF	FBgn0067783
Past1-PB	FBgn0016693
Cul2-PB	FBgn0032956
Tps1-PA	FBgn0027560
CG14483-PC	FBgn0034248
Ctr9-PA	FBgn0035205

Inx3-PA	FBgn0265274
Slik-PF	FBgn0035001
flr-PA	FBgn0260049
CG31368-PD	FBgn0051368
Usp2-PA	FBgn0031187
Pepck1-PA	FBgn0003067
Fmr1-PG	FBgn0028734
Arf79F-PC	FBgn0010348
CycB-PE	FBgn0000405
zip-PF	FBgn0265434
btz-PB	FBgn0045862
Not1-PG	FBgn0085436
IKKepsilon-PC	FBgn0086657
CalpA-PD	FBgn0012051
Meltrin-PD	FBgn0265140
lovit-PA	FBgn0267429
Moca-cyp-PA	FBgn0039581
Moe-PF	FBgn0011661
Drep2-PB	FBgn0028408
Usp2-PD	FBgn0031187
CG7632-PA	FBgn0037071
Klp10A-PE	FBgn0030268
SMC1-PA	FBgn0040283
Psi-PA	FBgn0014870
exd-PA	FBgn0000611
GckIII-PA	FBgn0266465
lqfR-PD	FBgn0261279
dnc-PJ	FBgn0000479
sxc-PA	FBgn0261403
par-1-PR	FBgn0260934
EMC1-PD	FBgn0037530
gb-PB	FBgn0039487
FoxK-PJ	FBgn0036134
hppy-PE	FBgn0263395
Zasp52-PW	FBgn0265991
Usp2-PE	FBgn0031187
Ntl-PA	FBgn0267326
zip-PG	FBgn0265434
CG4768-PB	FBgn0030790

crol-PE	FBgn0020309
su(f)-PE	FBgn0003559
rdx-PC	FBgn0264493
mthl10-PB	FBgn0035132
Sep2-PB	FBgn0014029
PDZ-GEF-PB	FBgn0265778
Blimp-1-PA	FBgn0035625
Alg-2-PC	FBgn0086378
PDZ-GEF-PC	FBgn0265778
mthl3-PC	FBgn0028956
CycB3-PA	FBgn0015625
BtbVII-PA	FBgn0263108
vap-PE	FBgn0003969
l(3)72Ab-PA	FBgn0263599
FoxK-PG	FBgn0036134
Ptpmeg2-PD	FBgn0028341
CG7546-PF	FBgn0035793
CycB3-PB	FBgn0015625
Sur-8-PB	FBgn0038504
Sep5-PA	FBgn0026361
Phax-PB	FBgn0033380
CG2017-PD	FBgn0037391
pnut-PB	FBgn0013726
Drep2-PD	FBgn0028408
eEF2-PC	FBgn0000559
Tmc-PC	FBgn0267796
btz-PC	FBgn0045862
mus301-PA	FBgn0002899
Upf1-PB	FBgn0030354
ple-PA	FBgn0005626
Inx2-PA	FBgn0027108
CG5171-PB	FBgn0031907
Hn-PA	FBgn0001208
CG4270-PA	FBgn0031407
Pp4-19C-PA	FBgn0023177
Cul1-PD	FBgn0015509
zip-PD	FBgn0265434
Poc1-PB	FBgn0036354
Meltrin-PC	FBgn0265140

IP3K2-PH	FBgn0283680
crol-PF	FBgn0020309
Phax-PA	FBgn0033380
IP3K2-PD	FBgn0283680
Drep2-PC	FBgn0028408
CG1129-PD	FBgn0037279
CG7546-PE	FBgn0035793
Sur-8-PE	FBgn0038504
crol-PB	FBgn0020309
Pepck2-PB	FBgn0034356
Slc45-1-PC	FBgn0035968
LpR2-PE	FBgn0051092
Not1-PD	FBgn0085436
DPCoAC-PA	FBgn0067783
Usp2-PH	FBgn0031187
Prp8-PA	FBgn0033688
mthl10-PD	FBgn0035132
lqfR-PC	FBgn0261279
vap-PA	FBgn0003969
mthl10-PE	FBgn0035132
SMC2-PA	FBgn0027783
hpo-PB	FBgn0261456
Sur-8-PA	FBgn0038504
Galphao-PH	FBgn0001122
Fmr1-PJ	FBgn0028734
Trh-PA	FBgn0035187
Inx2-PD	FBgn0027108
CG2852-PD	FBgn0034753
Zasp52-PK	FBgn0265991
Zasp52-PF	FBgn0265991
CG1542-PA	FBgn0039828
Hmg-2-PA	FBgn0026582
how-PE	FBgn0264491
Doa-PR	FBgn0265998
Slik-PE	FBgn0035001
Pvf1-PB	FBgn0030964
vap-PF	FBgn0003969
Ptpmeg2-PE	FBgn0028341
Zasp52-PT	FBgn0265991

CG8405-PB	FBgn0034071
Ntl-PB	FBgn0267326
FoxK-PI	FBgn0036134
CG8927-PC	FBgn0038405
btz-PA	FBgn0045862
CG2017-PB	FBgn0037391
CG17266-PA	FBgn0033089
btz-PD	FBgn0045862
Moe-PG	FBgn0011661
slbo-PB	FBgn0005638
mnd-PA	FBgn0002778
Psi-PB	FBgn0014870
Zasp52-PX	FBgn0265991
CG7840-PA	FBgn0032014
sens-2-PB	FBgn0051632
exd-PB	FBgn0000611
Ctr9-PB	FBgn0035205
CG16995-PA	FBgn0031412
CG7546-PB	FBgn0035793
MED1-PA	FBgn0037109
IP3K2-PA	FBgn0283680
mthl10-PA	FBgn0035132
Klp10A-PF	FBgn0030268
Epac-PG	FBgn0085421
wds-PA	FBgn0040066
Doa-PY	FBgn0265998
BtbVII-PE	FBgn0263108
Dab-PG	FBgn0000414
Snp-PF	FBgn0265192
su(f)-PF	FBgn0003559
Pp4-19C-PH	FBgn0023177
mmd-PG	FBgn0259110
Pp4-19C-PG	FBgn0023177
CG2017-PE	FBgn0037391
Adi1-PB	FBgn0052068
CalpA-PC	FBgn0012051
Cpr97Ea-PA	FBgn0039480
ebi-PA	FBgn0263933
Nle-PA	FBgn0021874

EMC1-PB	FBgn0037530
CG5171-PF	FBgn0031907
Blimp-1-PE	FBgn0035625
CG8005-PA	FBgn0035854
Fmr1-PK	FBgn0028734
Arpc2-PA	FBgn0032859
Pvf1-PA	FBgn0030964
BtbVII-PD	FBgn0263108
kraken-PB	FBgn0020545
Sc2-PA	FBgn0035471
Ptpmeg2-PH	FBgn0028341
Spn88Ea-PA	FBgn0028984
DNApol-theta-PA	FBgn0002905
Mtr4-PA	FBgn0001986
eEF2-PD	FBgn0000559
Fmr1-PD	FBgn0028734
EMC1-PA	FBgn0037530
Klp10A-PB	FBgn0030268
mio-PA	FBgn0031399
DPCoAC-PD	FBgn0067783
vap-PC	FBgn0003969
exd-PD	FBgn0000611
Galphao-PE	FBgn0001122
Meics-PB	FBgn0025874
hpo-PA	FBgn0261456
Cul1-PA	FBgn0015509
Arf79F-PI	FBgn0010348
IKKepsilon-PB	FBgn0086657
Pepck2-PA	FBgn0034356
CycB-PA	FBgn0000405
CG11309-PF	FBgn0037070
Cul1-PB	FBgn0015509
MED1-PB	FBgn0037109
Dab-PA	FBgn0000414
Dab-PF	FBgn0000414
su(f)-PG	FBgn0003559
CG9297-PE	FBgn0038181
Inx3-PB	FBgn0265274
PDZ-GEF-PA	FBgn0265778

Hn-PB	FBgn0001208
rdx-PA	FBgn0264493
CG2852-PA	FBgn0034753
IP3K2-PC	FBgn0283680
Moe-PD	FBgn0011661
kraken-PA	FBgn0020545
crol-PA	FBgn0020309
fliI-PA	FBgn0000709
EMC1-PC	FBgn0037530
Vps37B-PC	FBgn0037299
Inx2-PB	FBgn0027108
Snp-PG	FBgn0265192
mmd-PE	FBgn0259110
Doa-PP	FBgn0265998
Moe-PH	FBgn0011661
how-PF	FBgn0264491
Prp3-PB	FBgn0036915
dnc-PS	FBgn0000479
shakB-PA	FBgn0085387
Arf79F-PH	FBgn0010348
CG7504-PC	FBgn0035842
LpR2-PG	FBgn0051092
Zasp52-PZ	FBgn0265991
ps-PB	FBgn0261552
CG7504-PB	FBgn0035842
CG9899-PA	FBgn0034829
crol-PG	FBgn0020309
CG8927-PB	FBgn0038405
Sep1-PA	FBgn0011710
Slik-PA	FBgn0035001
lqf-PL	FBgn0028582
exd-PE	FBgn0000611
eEF2-PA	FBgn0000559
Not1-PE	FBgn0085436
Tmc-PD	FBgn0267796
CG14483-PB	FBgn0034248
Past1-PA	FBgn0016693
mnd-PC	FBgn0002778
CG17266-PB	FBgn0033089

slbo-PA	FBgn0005638
Cpr97Ea-PB	FBgn0039480
CG6841-PB	FBgn0036828
Galphao-PF	FBgn0001122
hppy-PB	FBgn0263395
modSP-PA	FBgn0051217
Blimp-1-PF	FBgn0035625
CG4270-PB	FBgn0031407
rdx-PE	FBgn0264493
FoxK-PH	FBgn0036134
mRpL48-PB	FBgn0031357
CG14483-PA	FBgn0034248
Ptpmeg2-PF	FBgn0028341
CG33158-PB	FBgn0053158
Ptpmeg2-PI	FBgn0028341
dnc-PD	FBgn0000479
Slc45-1-PD	FBgn0035968
rdx-PF	FBgn0264493
Clamp-PA	FBgn0032979
CG8005-PB	FBgn0035854
CG8405-PA	FBgn0034071
CG8578-PC	FBgn0030699
Slc45-1-PA	FBgn0035968
Spn88Ea-PB	FBgn0028984
CG8578-PA	FBgn0030699
CalpA-PB	FBgn0012051
Blimp-1-PD	FBgn0035625
how-PC	FBgn0264491
CG1161-PC	FBgn0037313
Spn38F-PB	FBgn0028986
mnd-PD	FBgn0002778
Sep4-PC	FBgn0259923
Vps37B-PB	FBgn0037299
CG5245-PA	FBgn0038047
obe-PA	FBgn0038344
CG4849-PA	FBgn0039566
MED1-PC	FBgn0037109
Sep4-PG	FBgn0259923
mmd-PB	FBgn0259110

CG9297-PD	FBgn0038181
Sep2-PA	FBgn0014029
CG5171-PE	FBgn0031907
Fmr1-PC	FBgn0028734
how-PD	FBgn0264491
mRpL48-PA	FBgn0031357
CG7546-PG	FBgn0035793
zip-PI	FBgn0265434
crol-PC	FBgn0020309
ps-PI	FBgn0261552
Galphao-PD	FBgn0001122
Inx2-PC	FBgn0027108
Klp10A-PC	FBgn0030268
Zasp52-PM	FBgn0265991
Not1-PF	FBgn0085436
par-1-PT	FBgn0260934
CG2017-PA	FBgn0037391
IKKbeta-PB	FBgn0024222
Meics-PA	FBgn0025874
CG31368-PC	FBgn0051368
CG34049-PB	FBgn0054049
CG1161-PA	FBgn0037313
Slik-PG	FBgn0035001
CG7632-PB	FBgn0037071
zip-PE	FBgn0265434
Arf79F-PJ	FBgn0010348
CG1129-PB	FBgn0037279
Slik-PB	FBgn0035001
Psi-PC	FBgn0014870
Snp-PE	FBgn0265192
Cul1-PC	FBgn0015509
Doa-PU	FBgn0265998
SMC3-PA	FBgn0015615
dnc-PI	FBgn0000479
sxc-PB	FBgn0261403
sens-2-PA	FBgn0051632
mthl10-PG	FBgn0035132
DPCoAC-PC	FBgn0067783
Hn-PC	FBgn0001208

Not1-PC	FBgn0085436
rasp-PA	FBgn0024194
how-PA	FBgn0264491
DAT-PA	FBgn0034136
wds-PB	FBgn0040066
CG31482-PA	FBgn0051482
Prp3-PA	FBgn0036915
CG13605-PB	FBgn0039150
Pvf1-PC	FBgn0030964
BtbVII-PB	FBgn0263108
CG8207-PA	FBgn0034035
LpR1-PH	FBgn0066101
Sep5-PB	FBgn0026361
lqf-PG	FBgn0028582
Zasp52-PQ	FBgn0265991
hth-PA	FBgn0001235
gb-PC	FBgn0039487
Moe-PI	FBgn0011661
LpR2-PC	FBgn0051092
vap-PB	FBgn0003969
CG4768-PC	FBgn0030790
Drep2-PA	FBgn0028408
CG7546-PD	FBgn0035793
Pp4-19C-PE	FBgn0023177
BtbVII-PG	FBgn0263108
DAT-PB	FBgn0034136
mthl3-PB	FBgn0028956
PDZ-GEF-PD	FBgn0265778
DPCoAC-PE	FBgn0067783
crol-PI	FBgn0020309
rdx-PB	FBgn0264493
Blimp-1-PC	FBgn0035625
CycB-PB	FBgn0000405
Spn28F-PA	FBgn0028987
CG1129-PA	FBgn0037279
Galphao-PG	FBgn0001122
CG2017-PC	FBgn0037391
Klp10A-PD	FBgn0030268
Spn38F-PA	FBgn0028986

Zasp52-PY	FBgn0265991
Pp4-19C-PI	FBgn0023177
mthl3-PA	FBgn0028956
CG8578-PB	FBgn0030699

Downregulated with increasing change in contraction amplitude in response to AST-C I:

Gene Name	FlyBase ID
Taf10-PA	FBpp0077401
CG4168-PC	FBpp0309808
CG41520-PA	FBpp0112834
CG42235-PB	FBpp0288580
chb-PA	FBpp0088470
beat-IIIa-PD	FBpp0292391
GluRIB-PD	FBpp0312406
CG8974-PD	FBpp0073973
sff-PB	FBpp0306195
CAP-PU	FBpp0297629
Lar-PH	FBpp0303683
Evi5-PB	FBpp0073391
Pdfr-PC	FBpp0309083
CG7889-PA	FBpp0074446
CG3655-PB	FBpp0112239
dpr14-PA	FBpp0071086
beat-IIIc-PA	FBpp0080524
Dhc36C-PB	FBpp0293284
Pdfr-PA	FBpp0099841
Shaw-PA	FBpp0088331
CARPB-PA	FBpp0071321
CG42788-PC	FBpp0292537
CG34133-PB	FBpp0110188
dpr6-PC	FBpp0303926
Ptp36E-PB	FBpp0310371
OXA1L-PA	FBpp0076001
Rsph1-PA	FBpp0080018
CG7920-PC	FBpp0306760
sli-PE	FBpp0303577
Shaw-PE	FBpp0304494

Mhcl-PG	FBpp0110274
RluA-1-PA	FBpp0079629
N-PB	FBpp0293201
MFS10-PB	FBpp0308734
wal-PB	FBpp0087187
CAP-PC	FBpp0087432
sca-PB	FBpp0086969
dpr6-PF	FBpp0311219
CG8974-PC	FBpp0073970
CG34126-PG	FBpp0303012
Diap1-PD	FBpp0305793
chp-PD	FBpp0303134
Mhcl-PC	FBpp0082686
Gfrl-PJ	FBpp0297313
nAChRalpha7-PD	FBpp0291048
CG6693-PB	FBpp0307760
Vha100-1-PE	FBpp0084750
CG16854-PD	FBpp0310216
CG3655-PC	FBpp0303757
CG34353-PC	FBpp0308425
Diap1-PF	FBpp0305795
CG14490-PA	FBpp0085980
CG3632-PI	FBpp0309796
Diap2-PA	FBpp0086431
DIP-delta-PD	FBpp0305788
Vha100-1-PB	FBpp0084744
Taf10b-PA	FBpp0077415
Ekar-PD	FBpp0311188
GluClalpha-PK	FBpp0307402
Culd-PB	FBpp0076398
CG7130-PA	FBpp0078137
Teh2-PB	FBpp0289848
Ptp36E-PA	FBpp0080614
Tret1-2-PA	FBpp0087180
Gfrl-PN	FBpp0311944
CG42235-PC	FBpp0288577
Trpgamma-PA	FBpp0080498
Toll-6-PA	FBpp0075367
AMPKalpha-PB	FBpp0070209

RluA-1-PB	FBpp0079630
CG10960-PA	FBpp0075675
Neto-PA	FBpp0308759
Culd-PC	FBpp0076399
CG6236-PA	FBpp0082576
Als2-PA	FBpp0078116
CG34126-PE	FBpp0303010
OXA1L-PB	FBpp0076000
LRP1-PF	FBpp0311204
wcy-PC	FBpp0293379
Ntan1-PD	FBpp0291076
Syt1-PE	FBpp0304523
Jhe-PB	FBpp0290965
Mhcl-PF	FBpp0110273
CG3339-PC	FBpp0271700
CG2924-PD	FBpp0311475
CG3655-PA	FBpp0070174
CG41520-PD	FBpp0291738
l(2)34Fd-PA	FBpp0080211
CG1674-PF	FBpp0290021
side-VIII-PD	FBpp0271792
side-VIII-PA	FBpp0111686
Wdr24-PC	FBpp0303329
Ppa-PB	FBpp0303282
CG8607-PA	FBpp0076548
CLS-PB	FBpp0084303
CG41520-PB	FBpp0112835
CG10737-PE	FBpp0099675
nAChRalpha7-PE	FBpp0291049
Smyd4-3-PA	FBpp0087232
CG4502-PB	FBpp0079044
beat-IIIc-PB	FBpp0080525
sff-PA	FBpp0088511
CG14894-PB	FBpp0307945
CG9003-PG	FBpp0303484
Lrp4-PC	FBpp0290880
CG4942-PA	FBpp0076251
CG34133-PE	FBpp0307012
sli-PD	FBpp0303576

beat-IIIa-PE	FBpp0309161
unc-45-PA	FBpp0081284
Gfrl-PF	FBpp0297309
CG1674-PK	FBpp0300429
CG8974-PA	FBpp0073971
Ppa-PA	FBpp0071835
Evi5-PE	FBpp0304866
Evi5-PA	FBpp0073392
CAP-PO	FBpp0289107
e-PA	FBpp0083505
CG34126-PD	FBpp0303009
Stip1-PA	FBpp0077790
chp-PC	FBpp0303133
Dhc62B-PC	FBpp0292225
Ance-PA	FBpp0080129
Ptp36E-PC	FBpp0310372
Tpr2-PD	FBpp0305671
Atg5-PA	FBpp0071023
nAChRalpha7-PA	FBpp0089248
Syt1-PH	FBpp0310442
shv-PA	FBpp0077720
dpr6-PA	FBpp0076082
Lrp4-PD	FBpp0309270
CARPB-PB	FBpp0298824
Teh2-PA	FBpp0073114
PPO2-PA	FBpp0087744
Amt-PB	FBpp0112150
cag-PA	FBpp0087334
GluRIB-PA	FBpp0303372
Csas-PB	FBpp0423255
tipE-PB	FBpp0073076
CG8281-PA	FBpp0076465
CG16854-PC	FBpp0298000
AMPKalpha-PC	FBpp0089374
dpr6-PE	FBpp0304912
CG1275-PA	FBpp0072785
CG11155-PD	FBpp0305854
CARPB-PC	FBpp0307860
Syt12-PA	FBpp0073598

tinc-PE	FBpp0293444
dpr7-PG	FBpp0306512
sli-PC	FBpp0303575
CG7920-PA	FBpp0084968
CG6414-PB	FBpp0401489
CG42788-PB	FBpp0292538
CG7675-PD	FBpp0310903
Lsp1beta-PB	FBpp0311765
ND-B17-PC	FBpp0310296
Clamp-PB	FBpp0099821
dpr7-PF	FBpp0306511
schlank-PB	FBpp0070899
dpr14-PB	FBpp0298271
Atg14-PA	FBpp0084739
wds-PA	FBpp0070422
Lsp1beta-PA	FBpp0077690
wcy-PF	FBpp0302662
Cht2-PA	FBpp0072677
dpr20-PA	FBpp0072491
CG32590-PA	FBpp0073805
crb-PB	FBpp0110307
CG13630-PA	FBpp0084120
CG5037-PA	FBpp0079582
fal-PD	FBpp0312519
MFS10-PA	FBpp0073555
CG1674-PH	FBpp0290022
CG6693-PA	FBpp0081843
RluA-1-PC	FBpp0079631
CG10444-PA	FBpp0085617
Trpgamma-PB	FBpp0080499
Jhe-PC	FBpp0309035
HERC2-PC	FBpp0290558
Ntan1-PA	FBpp0085839
Diap1-PE	FBpp0305794
CG1674-PE	FBpp0290020
CG11710-PA	FBpp0088586
wcy-PG	FBpp0303447
crb-PC	FBpp0293268
side-VIII-PB	FBpp0111687

CLS-PA	FBpp0084304
Smyd4-4-PA	FBpp0087091
Vha100-1-PK	FBpp0307388
SmydA-2-PA	FBpp0074807
CG1275-PD	FBpp0072786
nAChRalpha6-PH	FBpp0303720
fal-PC	FBpp0302865
CG1275-PC	FBpp0072784
PPO3-PA	FBpp0291496
nAChRalpha7-PF	FBpp0310357
mio-PA	FBpp0077507
nAChRalpha2-PB	FBpp0084024
rgn-PB	FBpp0301169
CG4502-PA	FBpp0079045
CG1674-PJ	FBpp0290024
CG5757-PB	FBpp0303030
CARPA-PC	FBpp0310005
Evi5-PD	FBpp0289957
Sbf-PB	FBpp0082004
Neto-PB	FBpp0308760
Tollo-PA	FBpp0075360
CG3036-PB	FBpp0307796
Pdfr-PD	FBpp0309084
GluClalpha-PN	FBpp0310353
CG11384-PA	FBpp0070241
Dhc16F-PA	FBpp0074283
sca-PA	FBpp0086968
Gfrl-PG	FBpp0297310
unc-45-PB	FBpp0312575
DIP-zeta-PC	FBpp0292884
Shaw-PC	FBpp0288427
Syt12-PB	FBpp0303988
chb-PC	FBpp0088471
CG15436-PA	FBpp0077132
Lrp4-PB	FBpp0073931
SmydA-4-PB	FBpp0073247
CG34353-PB	FBpp0293835
Ance-PB	FBpp0080130
sut4-PA	FBpp0088616

CG11155-PA	FBpp0088259
CG7675-PA	FBpp0083002
Teh1-PA	FBpp0081629
fal-PB	FBpp0288723
Ccn-PB	FBpp0074951
SmydA-5-PA	FBpp0085358
schlank-PA	FBpp0070898
CG7675-PE	FBpp0310904
CG11044-PA	FBpp0085623
CAP-PK	FBpp0289103
CG8974-PE	FBpp0073974
CG7675-PB	FBpp0083003
Vha100-1-PG	FBpp0084746
sli-PB	FBpp0303574
Shaw-PD	FBpp0304493
CG34126-PF	FBpp0303011
CG10737-PO	FBpp0288756
Cht2-PC	FBpp0306200
tinc-PF	FBpp0307967
CG3036-PA	FBpp0077083
Mhcl-PI	FBpp0304712
CLS-PD	FBpp0303777
side-VI-PC	FBpp0290292
chb-PB	FBpp0088469
Ir8a-PA	FBpp0071268
CG11178-PB	FBpp0073636
CG10737-PV	FBpp0309393
CG11178-PC	FBpp0311349
tinc-PA	FBpp0088712
Ekar-PB	FBpp0110206
CG33926-PB	FBpp0311233
CG3655-PD	FBpp0303758
CG1275-PB	FBpp0072783
CG6414-PA	FBpp0070594
Clamp-PA	FBpp0085317
Dnah3-PD	FBpp0288420
CG11710-PB	FBpp0088585
DIP-epsilon-PA	FBpp0289244
nemy-PL	FBpp0308789

CG34353-PA	FBpp0111475
Cht9-PA	FBpp0071471
crol-PH	FBpp0307450
chp-PF	FBpp0307394
CG16854-PB	FBpp0293128
CG5757-PA	FBpp0085966
Ntan1-PB	FBpp0085840
CG34133-PC	FBpp0290295
ND-B17-PA	FBpp0080329
Vps50-PA	FBpp0086024
GluRIB-PC	FBpp0306805
CG6236-PB	FBpp0082575
CG43055-PA	FBpp0293179
Wdr24-PB	FBpp0084909
CAP-PF	FBpp0087431
tinc-PG	FBpp0307968
CG2924-PB	FBpp0290017
Ance-3-PB	FBpp0099733
Culd-PA	FBpp0076397
Pdfr-PB	FBpp0300789
CG3632-PG	FBpp0111903
crb-PD	FBpp0306945
Toll-7-PA	FBpp0085638
Xpd-PA	FBpp0071503
Cht2-PB	FBpp0297108
dpr6-PD	FBpp0304911
Sbf-PA	FBpp0082003
crol-PC	FBpp0079847
Dh44-R2-PB	FBpp0111988
sff-PC	FBpp0306196
CG2924-PE	FBpp0312228
Ance-PC	FBpp0310259
cag-PB	FBpp0304270
CG42235-PA	FBpp0288581
trpl-PD	FBpp0290876
CG7675-PC	FBpp0083004
side-VIII-PE	FBpp0309581
CG32085-PA	FBpp0075864
beat-IIIb-PD	FBpp0303008

CG15390-PA	FBpp0077444
wcy-PA	FBpp0074186
CARPB-PD	FBpp0311998
Trpgamma-PD	FBpp0307143
Evi5-PC	FBpp0289956
CG10960-PC	FBpp0075673
CG6723-PA	FBpp0081881
GluClalpha-PP	FBpp0310355
Shaw-PB	FBpp0088332
DIP-zeta-PB	FBpp0079377
Gfrl-PL	FBpp0303066
GluClalpha-PH	FBpp0307399
Smyd4-2-PA	FBpp0075717
CG3632-PH	FBpp0111904
GluRIB-PB	FBpp0303373
crb-PA	FBpp0083987
CLS-PC	FBpp0084305
GluClalpha-PL	FBpp0307403
LRP1-PG	FBpp0311205
Vha100-1-PD	FBpp0084749
Diap2-PB	FBpp0086432
wds-PB	FBpp0300790
Lar-PI	FBpp0303684
Ance-3-PC	FBpp0310234
SmydA-4-PA	FBpp0073246
Toll-6-PC	FBpp0297411
Ppa-PC	FBpp0309766
rgn-PC	FBpp0305577
Mhcl-PD	FBpp0082687
MFS10-PC	FBpp0308735
Syt1-PI	FBpp0311487
klg-PA	FBpp0083730
wal-PA	FBpp0087186
CG34126-PB	FBpp0288449
Grik-PC	FBpp0307023
SmydA-3-PE	FBpp0304342
tinc-PB	FBpp0088713
side-VI-PB	FBpp0110105
Jhe-PA	FBpp0086362

Cht8-PA	FBpp0071463
Ntan1-PC	FBpp0291075
CG7166-PC	FBpp0305585
CG33926-PA	FBpp0091164
CG10737-PS	FBpp0288752
CG10960-PB	FBpp0075674
CG10737-PX	FBpp0309395
wcy-PD	FBpp0293380
CG42324-PF	FBpp0303175
CG4168-PB	FBpp0294010
PPO1-PA	FBpp0291497
Toll-6-PB	FBpp0297410
sli-PF	FBpp0303578
CG14894-PA	FBpp0082765
CG8974-PB	FBpp0073972
CG11710-PC	FBpp0308739
DIP-delta-PE	FBpp0305789
trp-PA	FBpp0084879
Teh1-PB	FBpp0303115

Appendix B: GO Term Analysis of Differentially Expressed Transcripts

GO Terms returned from analysis of positively-correlated transcripts (upregulated with increasing change in contraction amplitude in response to AST-C I):

GO biological process	Fold Enrichment	Raw p-value
glycerol biosynthetic process (GO:0006114)	88.25	7.37E-04
glycerol biosynthetic process from pyruvate (GO:0046327)	88.25	7.37E-04
propionate catabolic process (GO:0019543)	88.25	7.37E-04
propionate metabolic process (GO:0019541)	88.25	7.37E-04
alditol biosynthetic process (GO:0019401)	88.25	7.37E-04
trehalose biosynthetic process (GO:0005992)	58.83	1.22E-03
oenocyte development (GO:0007438)	33.09	2.13E-04
oenocyte differentiation (GO:0001742)	32.09	1.88E-05
intercellular transport (GO:0010496)	29.42	2.82E-04
axon ensheathment (GO:0008366)	24.07	4.59E-04
pole plasm protein localization (GO:0007318)	22.06	5.69E-04
ensheathment of neurons (GO:0007272)	18.91	8.36E-04
cellular carbohydrate biosynthetic process (GO:0034637)	17.65	1.35E-04
positive regulation of JNK cascade (GO:0046330)	11.77	5.41E-04
positive regulation of stress-activated MAPK cascade (GO:0032874)	11.03	6.76E-04
positive regulation of stress-activated protein kinase signaling cascade (GO:0070304)	11.03	6.76E-04
positive regulation of proteasomal protein catabolic process (GO:1901800)	10.7	7.51E-04
activation of protein kinase activity (GO:0032147)	10.7	7.51E-04
signal transduction by protein phosphorylation (GO:0023014)	10.51	1.74E-04
oocyte fate determination (GO:0030716)	10.09	9.19E-04
stress-activated protein kinase signaling cascade (GO:0031098)	9.81	1.01E-03
positive regulation of proteolysis involved in cellular protein catabolic process (GO:1903052)	9.81	1.01E-03
myofibril assembly (GO:0030239)	9.59	2.57E-04
imaginal disc-derived wing hair organization (GO:0035317)	9.39	2.81E-04
mitotic cytokinesis (GO:0000281)	9.22	1.86E-05
non-sensory hair organization (GO:0035316)	9.19	3.08E-04
hair cell differentiation (GO:0035315)	9.19	3.08E-04

positive regulation of cellular protein catabolic process (GO:1903364)	9.05	1.33E-03
presynaptic endocytosis (GO:0140238)	9.05	1.33E-03
synaptic vesicle endocytosis (GO:0048488)	9.05	1.33E-03
regulation of proteolysis involved in cellular protein catabolic process (GO:1903050)	9.01	3.36E-04
organic hydroxy compound biosynthetic process (GO:1901617)	8.97	8.60E-05
regulation of cellular protein catabolic process (GO:1903362)	8.49	4.34E-04
cytoskeleton-dependent cytokinesis (GO:0061640)	8.49	5.86E-07
epidermal cell differentiation (GO:0009913)	8.49	4.34E-04
cytokinesis (GO:0000910)	8.4	6.36E-07
regulation of alternative mRNA splicing, via spliceosome (GO:0000381)	7.93	1.29E-05
positive regulation of apoptotic process (GO:0043065)	7.56	2.06E-04
striated muscle cell development (GO:0055002)	7.23	8.54E-04
positive regulation of proteolysis (GO:0045862)	7.16	2.73E-04
muscle cell development (GO:0055001)	7.12	9.14E-04
regulation of JNK cascade (GO:0046328)	7.12	9.14E-04
epidermis development (GO:0008544)	7	9.78E-04
regulation of mRNA processing (GO:0050684)	6.91	1.05E-05
positive regulation of programmed cell death (GO:0043068)	6.86	1.07E-04
regulation of mRNA splicing, via spliceosome (GO:0048024)	6.85	3.45E-05
regulation of RNA splicing (GO:0043484)	6.85	1.12E-05
regulation of stress-activated MAPK cascade (GO:0032872)	6.79	1.12E-03
regulation of stress-activated protein kinase signaling cascade (GO:0070302)	6.79	1.12E-03
regulation of mRNA metabolic process (GO:1903311)	6.49	5.61E-06
border follicle cell migration (GO:0007298)	6.24	1.87E-04
positive regulation of cell death (GO:0010942)	6.18	1.98E-04
regulation of proteolysis (GO:0030162)	6.17	8.51E-06
positive regulation of cellular catabolic process (GO:0031331)	6	2.35E-04
regulation of protein kinase activity (GO:0045859)	5.76	8.10E-04
striated muscle cell differentiation (GO:0051146)	5.76	8.10E-04
establishment of tissue polarity (GO:0007164)	5.52	9.99E-04

establishment of planar polarity (GO:0001736)	5.52	9.99E-04
ovarian follicle cell migration (GO:0007297)	5.47	4.00E-04
negative regulation of intracellular signal transduction (GO:1902532)	5.35	1.16E-03
positive regulation of protein modification process (GO:0031401)	5.28	3.03E-05
positive regulation of protein phosphorylation (GO:0001934)	5.28	4.88E-04
positive regulation of catabolic process (GO:0009896)	5.24	5.12E-04
regulation of reproductive process (GO:2000241)	5.15	5.63E-04
import into cell (GO:0098657)	4.9	1.31E-04
positive regulation of cellular protein metabolic process (GO:0032270)	4.76	1.03E-06
RNA splicing (GO:0008380)	4.73	1.39E-05
cell division (GO:0051301)	4.66	6.93E-06
mRNA processing (GO:0006397)	4.64	3.17E-06
positive regulation of multi-organism process (GO:0043902)	4.64	4.40E-04
negative regulation of signal transduction (GO:0009968)	4.61	6.57E-07
regulation of protein phosphorylation (GO:0001932)	4.6	4.06E-05
mRNA splicing, via spliceosome (GO:0000398)	4.58	4.23E-05
RNA splicing, via transesterification reactions with bulged adenosine as nucleophile (GO:0000377)	4.58	4.23E-05
RNA splicing, via transesterification reactions (GO:0000375)	4.54	4.59E-05
regulation of apoptotic process (GO:0042981)	4.53	1.04E-04
positive regulation of protein metabolic process (GO:0051247)	4.52	1.92E-06
positive regulation of phosphorylation (GO:0042327)	4.48	1.23E-03
regulation of programmed cell death (GO:0043067)	4.35	6.55E-05
ameboidal-type cell migration (GO:0001667)	4.25	7.65E-04
negative regulation of cell communication (GO:0010648)	4.25	1.83E-06
supramolecular fiber organization (GO:0097435)	4.25	3.63E-04
negative regulation of signaling (GO:0023057)	4.24	1.89E-06
mRNA metabolic process (GO:0016071)	4.21	2.04E-06
regulation of cell death (GO:0010941)	4.12	5.05E-05

locomotory behavior (GO:0007626)	4.01	1.10E-03
axis specification (GO:0009798)	4.01	1.10E-03
regulation of cellular catabolic process (GO:0031329)	4.01	5.41E-04
regulation of mitotic cell cycle (GO:0007346)	3.95	6.00E-04
negative regulation of response to stimulus (GO:0048585)	3.94	4.62E-06
regulation of protein modification process (GO:0031399)	3.94	9.43E-06
regulation of multi-organism process (GO:0043900)	3.93	1.56E-04
blastoderm segmentation (GO:0007350)	3.92	1.26E-03
regulation of phosphorylation (GO:0042325)	3.91	1.61E-04
developmental maturation (GO:0021700)	3.88	1.35E-03
muscle structure development (GO:0061061)	3.86	7.10E-04
imaginal disc-derived wing morphogenesis (GO:0007476)	3.81	1.04E-04
regulation of cellular protein metabolic process (GO:0032268)	3.73	2.10E-08
positive regulation of signal transduction (GO:0009967)	3.73	9.20E-06
wing disc development (GO:0035220)	3.67	1.11E-05
wing disc morphogenesis (GO:0007472)	3.66	1.47E-04
actin cytoskeleton organization (GO:0030036)	3.63	5.65E-04
regulation of catabolic process (GO:0009894)	3.59	1.14E-03
regulation of intracellular signal transduction (GO:1902531)	3.57	9.86E-05
regulation of protein metabolic process (GO:0051246)	3.57	4.85E-08
regulation of cell cycle (GO:0051726)	3.52	1.14E-04
anatomical structure formation involved in morphogenesis (GO:0048646)	3.51	8.40E-07
positive regulation of developmental process (GO:0051094)	3.5	4.01E-04
positive regulation of multicellular organismal process (GO:0051240)	3.48	4.26E-04
positive regulation of cell communication (GO:0010647)	3.44	2.41E-05
positive regulation of signaling (GO:0023056)	3.44	2.41E-05
morphogenesis of an epithelium (GO:0002009)	3.42	3.75E-07
positive regulation of response to stimulus (GO:0048584)	3.41	4.30E-06
regulation of signal transduction (GO:0009966)	3.41	1.77E-08

regulation of phosphate metabolic process (GO:0019220)	3.41	5.05E-04
regulation of phosphorus metabolic process (GO:0051174)	3.41	5.05E-04
regulation of response to stress (GO:0080134)	3.38	5.35E-04
imaginal disc-derived appendage development (GO:0048737)	3.36	1.76E-04
actin filament-based process (GO:0030029)	3.36	1.01E-03
embryo development (GO:0009790)	3.35	5.69E-06
cell motility (GO:0048870)	3.33	3.42E-04
appendage development (GO:0048736)	3.33	1.96E-04
oogenesis (GO:0048477)	3.32	1.08E-06
tissue morphogenesis (GO:0048729)	3.32	6.21E-07
protein phosphorylation (GO:0006468)	3.31	1.13E-03
central nervous system development (GO:0007417)	3.28	1.19E-03
localization of cell (GO:0051674)	3.27	4.03E-04
post-embryonic appendage morphogenesis (GO:0035120)	3.26	4.14E-04
tube development (GO:0035295)	3.25	1.57E-07
cell migration (GO:0016477)	3.23	1.33E-03
regulation of cell differentiation (GO:0045595)	3.2	9.55E-05
female gamete generation (GO:0007292)	3.18	1.27E-06
imaginal disc-derived appendage morphogenesis (GO:0035114)	3.17	5.23E-04
imaginal disc development (GO:0007444)	3.17	6.96E-06
appendage morphogenesis (GO:0035107)	3.14	5.65E-04
cell fate commitment (GO:0045165)	3.14	9.61E-04
tube morphogenesis (GO:0035239)	3.1	2.72E-05
regulation of cell development (GO:0060284)	3.09	6.57E-04
regionalization (GO:0003002)	3.08	8.59E-05
regulation of multicellular organismal development (GO:2000026)	3.06	1.12E-05
regulation of catalytic activity (GO:0050790)	3.05	4.36E-04
epithelium development (GO:0060429)	3.04	1.15E-08
epithelial tube morphogenesis (GO:0060562)	2.99	1.18E-04
response to abiotic stimulus (GO:0009628)	2.97	3.41E-04
germ cell development (GO:0007281)	2.96	2.38E-06
animal organ development (GO:0048513)	2.95	8.30E-10
regulation of cell communication (GO:0010646)	2.94	3.46E-07
regulation of signaling (GO:0023051)	2.94	3.46E-07

positive regulation of metabolic process (GO:0009893)	2.9	1.61E-07
gamete generation (GO:0007276)	2.89	1.81E-07
developmental process involved in reproduction (GO:0003006)	2.88	3.26E-07
post-embryonic animal organ morphogenesis (GO:0048563)	2.87	7.64E-04
imaginal disc morphogenesis (GO:0007560)	2.87	7.64E-04
eye development (GO:0001654)	2.85	1.29E-03
visual system development (GO:0150063)	2.85	1.29E-03
sensory system development (GO:0048880)	2.85	1.29E-03
regulation of response to stimulus (GO:0048583)	2.85	2.43E-07
regulation of developmental process (GO:0050793)	2.84	4.95E-06
pattern specification process (GO:0007389)	2.83	2.17E-04
positive regulation of nitrogen compound metabolic process (GO:0051173)	2.82	3.33E-06
positive regulation of cellular metabolic process (GO:0031325)	2.82	1.28E-06
multicellular organismal reproductive process (GO:0048609)	2.8	7.77E-08
cellular process involved in reproduction in multicellular organism (GO:0022412)	2.8	1.46E-06
metamorphosis (GO:0007552)	2.79	3.94E-04
multi-organism reproductive process (GO:0044703)	2.78	8.87E-08
sexual reproduction (GO:0019953)	2.78	8.87E-08
tissue development (GO:0009888)	2.78	9.26E-08
animal organ morphogenesis (GO:0009887)	2.78	1.11E-05
mitotic cell cycle (GO:0000278)	2.76	1.06E-03
instar larval or pupal morphogenesis (GO:0048707)	2.76	6.81E-04
regulation of molecular function (GO:0065009)	2.74	7.41E-04
positive regulation of macromolecule metabolic process (GO:0010604)	2.69	7.31E-06
post-embryonic animal morphogenesis (GO:0009886)	2.68	9.11E-04
post-embryonic animal organ development (GO:0048569)	2.67	9.29E-04
sensory organ development (GO:0007423)	2.66	9.68E-04
RNA processing (GO:0006396)	2.65	4.34E-04
positive regulation of biological process (GO:0048518)	2.64	1.21E-10

reproductive process (GO:0022414)	2.62	1.44E-07
multicellular organism reproduction (GO:0032504)	2.59	7.53E-08
anatomical structure morphogenesis (GO:0009653)	2.58	5.24E-09
cell cycle (GO:0007049)	2.56	2.90E-04
regulation of multicellular organismal process (GO:0051239)	2.56	5.87E-05
positive regulation of cellular process (GO:0048522)	2.55	1.16E-08
multi-organism process (GO:0051704)	2.54	3.14E-08
cell development (GO:0048468)	2.52	1.54E-07
system development (GO:0048731)	2.48	3.60E-09
reproduction (GO:0000003)	2.46	1.50E-07
cellular developmental process (GO:0048869)	2.38	2.40E-08
response to stress (GO:0006950)	2.35	1.23E-05
nervous system development (GO:0007399)	2.34	2.83E-05
RNA metabolic process (GO:0016070)	2.34	2.59E-04
cell differentiation (GO:0030154)	2.33	1.37E-07
regulation of nitrogen compound metabolic process (GO:0051171)	2.29	2.51E-08
multicellular organism development (GO:0007275)	2.28	3.89E-10
response to external stimulus (GO:0009605)	2.27	1.70E-04
anatomical structure development (GO:0048856)	2.27	5.36E-12
neurogenesis (GO:0022008)	2.27	2.50E-04
regulation of primary metabolic process (GO:0080090)	2.26	3.55E-08
regulation of macromolecule metabolic process (GO:0060255)	2.24	1.73E-08
developmental process (GO:0032502)	2.24	3.36E-12
cellular component assembly (GO:0022607)	2.23	2.47E-04
regulation of cellular metabolic process (GO:0031323)	2.17	8.15E-08
generation of neurons (GO:0048699)	2.17	1.20E-03
negative regulation of cellular process (GO:0048523)	2.16	5.95E-05
regulation of metabolic process (GO:0019222)	2.15	2.98E-08
cellular component biogenesis (GO:0044085)	2.15	1.23E-04
gene expression (GO:0010467)	2.1	3.11E-04
cellular localization (GO:0051641)	2.08	1.17E-03
cellular response to stimulus (GO:0051716)	2.06	6.54E-05

regulation of biological process (GO:0050789)	2.02	8.50E-14
multicellular organismal process (GO:0032501)	2.01	1.28E-11
negative regulation of biological process (GO:0048519)	1.99	1.69E-04
protein modification process (GO:0036211)	1.99	1.01E-03
cellular protein modification process (GO:0006464)	1.99	1.01E-03
regulation of cellular process (GO:0050794)	1.96	2.79E-11
biological regulation (GO:0065007)	1.89	1.04E-12
regulation of gene expression (GO:0010468)	1.86	5.35E-04
localization (GO:0051179)	1.83	3.81E-05
response to stimulus (GO:0050896)	1.73	4.74E-05
cellular process (GO:0009987)	1.5	1.31E-09
macromolecule metabolic process (GO:0043170)	1.49	1.25E-03
primary metabolic process (GO:0044238)	1.43	1.29E-03
biological process (GO:0008150)	1.14	1.69E-04

GO Terms returned from analysis of negatively-correlated transcripts (upregulated with decreasing change in contraction amplitude in response to AST-C I):

GO biological process	Fold Enrichment	Raw p-value
manganese ion transport (GO:0006828)	73.23	3.47E-05
dopamine metabolic process (GO:0042417)	30.04	2.17E-05
catecholamine metabolic process (GO:0006584)	26.04	3.49E-05
catechol-containing compound metabolic process (GO:0009712)	26.04	3.49E-05
cilium movement (GO:0003341)	16.27	2.53E-05
synapse organization (GO:0050808)	7.09	7.44E-08
response to external stimulus (GO:0009605)	2.83	1.03E-06
response to stimulus (GO:0050896)	1.84	1.61E-05
cellular process (GO:0009987)	1.47	9.42E-08

Appendix C: Differentially Expressed Genes & Potential Interventions

Gene/Protein	Up or downregulated? (log2FoldChange, adjusted p-value)	GO Term	Function	Pharmaceutical Intervention
Alg-2 ortholog (FBgn0086378)	+ (0.017, 0.099)	Positive regulation of stress-activated MAPK cascade/JNK cascade	Calcium ion binding, positive regulation of JNK cascade	N/A
Pvf1 ortholog (LD28763p) (FBgn0030964)	+ (0.037, 0.071)	Positive regulation of stress-activated MAPK cascade/JNK cascade	Binds to and activates the receptor tyrosine kinase encoded by Pvr; activates MAPK and JNK cascades among others	N/A
Hppy ortholog (Happyhour, isoform A) (FBgn0263395)	+ (0.015, 0.077)	Positive regulation of stress-activated MAPK cascade/JNK cascade; Activation of protein kinase activity	Ser/Thr Kinase from Germinal Center Kinase I family, linked to Egfr, Hippo, and Tor pathways	erlotinib and gefitinib are two EGFR pathway inhibitors that have been effective in *Drosophila* (Corl et al., 2009)
Rdx ortholog (Protein roadkill) (FBgn0264493)	+ (0.014, 0.078)	Positive regulation of stress-activated MAPK cascade/JNK cascade	substrate recognition component of Cul3-based E3 ubiquitin ligase complexes; negative regulator of Hedgehog signaling pathway	N/A

Gene/Protein	Up or downregulated? (log2FoldChange, adjusted p-value)	GO Term	Function	Pharmaceutical Intervention
Serine/threonine protein kinase hippo (hpo) (FBgn0261456)	+ (0.015, 0.077)	Activation of protein kinase activity	Kinase, STE20 subfamily, Germinal center kinase, hippo pathway	N/A
Slik- Sterile 20-like kinase, isoform B (FBgn0035001)	+ (0.013, 0.087)	Activation of protein kinase activity	Serine/threonine kinase activity, Germinal center kinase (characterized by N term STE20 kinase domain)	N/A
Gck III ortholog (FBgn0266465)	+ (0.015, 0.077)	Activation of protein kinase activity	Member of STE20 superfamily, only *Drosophila* GCK type 3 family member, serine/threonine kinase	N/A
I-kappaB kinase beta (FBgn0024222)	+ (0.015, 0.048)	Negative regulation of intracellular signal transduction	Activation of transcription factor encoded by Rel, serine/threonine kinase, stress response	N/A

Gene/Protein	Up or downregulated? (log2FoldChange, adjusted p-value)	GO Term	Function	Pharmaceutical Intervention
Par-1 (FBgn0260934)	+ (0.015, 0.048)	Negative regulation of intracellular signal transduction	Non-specific serine/threonine protein kinase, negatively regulates Hippo signaling, calcium/calmodulin dependent protein kinase	N/A
dunce (FBgn0000479)	+ (0.038, 0.094)	Negative regulation of intracellular signal transduction	cAMP specific cyclic phosphodiesterase isoform I, functions in neurological plasticity/synapse development and function	Forskolin (adenylyl cyclase activator) to counteract (Bhattacharya et al., 1999)
Cullin homolog 1 (FBgn0015509)	+ (0.013, 0.066)	Negative regulation of intracellular signal transduction	Ubiquitin protein ligase binding activity	N/A
ebi (FBgn0263933)	+ (0.010, 0.068)	Negative regulation of intracellular signal transduction	Regulates EGFR, notch, Wg signaling pathways	N/A

Gene/Protein	Up or downregulated? (log2FoldChange, adjusted p-value)	GO Term	Function	Pharmaceutical Intervention
Vap (FBgn0003969)	+ (0.014, 0.052)	Negative regulation of intracellular signal transduction	GTPase activating protein for Ras family small GTPases; Ras-MAP kinase pathway; EGF receptor pathway	N/A
G_o protein alpha subunit (FBgn0001122)	+ (0.018, 0.079)	Central nervous system development	G-protein	Pertussis toxin (PTX) selectively inhibits G_o signaling (Ferris et al., 2006)
Transient receptor potential protein (FBpp0084879, FBpp0290876, FBpp0080498, FBpp0080499)	- (-0.036, 0.053)	Manganese ion transport; response to external stimulus	Non-selective cation channel; high Ca permeability; function in a variety of pathways including Ca^{2+} and Mg^{2+} homeostasis (Minke, 2010)	TRP channels have been shown to be blocked by lanthanum (La^{3+}) in *Drosophila* (Hardie and Minke, 1992)
Protein tyrosine phosphatase 36E (FBpp0310372, FBpp0310371, FBpp0080614)	- (-0.017, 0.048)	Response to external stimulus	Tyrosine-specific protein phosphatase	N/A

Gene/Protein	Up or downregulated? (log2FoldChange, adjusted p-value)	GO Term	Function	Pharmaceutical Intervention
AMP-activated protein kinase alpha subunit (FBpp0070209, FBpp0089374)	- (-0.035, 0.072)	Response to external stimulus	Serine/threonine kinase activity; usually active when TOR pathway is inhibited (stress responsive inhibitor of TOR); important for stress survival and longevity; activated upon energy depletion	Sestrins activate AMPK as feedback inhibitor of TOR; single sestrin ortholog in *Drosophila* (Lee et al., 2010)
Toll-like receptor 6 (FBpp0297410, FBpp0075367, FBpp0297411)	- (-0.023, 0.083)	Response to external stimulus	Neurotrophin receptor activity; contributes to dendritic guidance; activation of NF-κB is target of Toll pathway	Spatzle activates the Toll pathway; *Drosophila* IκB factor Cactus typically inhibits NF-κB
Toll-like receptor 7 (FBpp0085638)	- (-0.023, 0.083)	Response to external stimulus	Anti-viral defenses; activation of NF-κB is target of Toll pathway	Same as above
Toll-like receptor Tollo (FBpp0075360)	- (-0.023, 0.083)	Response to external stimulus	Innate immune response; reg. of glucose metabolism; protein glycosylation; peripheral NS development; interacts with Toll 6; activation of NF-κB is target of Toll pathway	Same as above

Gene/Protein	Up or downregulated? (log2FoldChange, adjusted p-value)	GO Term	Function	Pharmaceutical Intervention
Notch (Neurogenic locus notch protein) (FBpp0293201)	- (-0.035, 0.053)	Response to external stimulus	Chromatin binding activity; transmembrane signaling receptor activity; involved in organ development, neurogenesis	Notch receptor is activated by binding of Delta (DI) or Serrate (ser)
Sugar-free frosting isoform A (FBpp0088511)	- (-0.035, 0.072)	Synapse organization	Tau protein kinase activity; serine/threonine kinase activity; NMJ development; protein N-glycosylation; calcium/calmodulin dependent kinase	N/A
DPR-interacting protein delta-CTX related type 1 transmembrane protein (FBpp0305788, FBpp0305789)	- (-0.028, 0.094)	Synapse organization	Localizes to integral component of plasma membrane; involved in synapse organization	N/A

Gene/Protein	Up or downregulated? (log2FoldChange, adjusted p-value)	GO Term	Function	Pharmaceutical Intervention
Klingon (FBpp0083730)	- (-0.026, 0.081)	Synapse organization	Homophilic cell adhesion molecule regulated by Notch signaling; axon guidance receptor activity	N/A
Neto ortholog (FBpp0308760)	- (-0.035, 0.071)	Synapse organization	Transmembrane protein; associates with ionotropic glutamate receptors and modulates subcellular distribution and function	N/A
Lrp4 ortholog (FBpp0073931)	- (-0.023, 0.056)	Synapse organization	Type I transmembrane protein; enriched in presynaptic terminals; calcium ion binding activity; required for NMJ formation	N/A